Doctoral school in natural sciences dissertation series
University of Helsinki

1/2020

ADVANCED OXIDATION TECHNIQUES AND INORGANIC SORBENT MATERIALS IN THE REMOVAL OF RADIOACTIVE COBALT FROM AQUEOUS NUCLEAR WASTE

Leena Malinen

Department of Chemistry - Radiochemistry
Faculty of Science
University of Helsinki
Finland

ACADEMIC DISSERTATION

To be presented, with the permission of the Faculty of Science of the University of Helsinki, for public examination streamed from University premises, on 29th May 2020, at 14 o'clock.

Helsinki 2020

Supervisor

Senior Lecturer, Professor (H.C.) Risto Harjula
Ion-Exchange for Nuclear Waste Treatment and for Recycling
Department of Chemistry - Radiochemistry
University of Helsinki, Finland

Pre-examiners

Professor Ulla Lassi
Research unit of Sustainable Chemistry
University of Oulu, Finland

Doctor Nick Evans
Department of Chemistry and Forensics
Nottingham Trent University, United Kingdom

Dissertation opponent

Professor Sarah Heath
University of Manchester, United Kingdom

ISBN 978-951-51-5987-8 (PRINT)
ISBN 978-951-51-5988-5 (ONLINE)
ISSN 2669-882X (PRINT)
ISSN 2670-2010 (ONLINE)
http://ethesis.helsinki.fi/

Unigrafia
Helsinki 2020

use creative imagination as a force in your life,
the support from others as a strength

and you'll be able to see beyond challenges,
obtain the result you dared to dream

L. Malinen

ABSTRACT

During the operation of nuclear power plants, the plant's reactor materials can be corroded. In the prevailing conditions, the corrosion products are activated. This results in radiation background which should be minimized in order to protect the plant personnel. One of the most harmful radionuclides responsible for the radiation exposure is ^{60}Co due to its relatively long half-life and high gamma decay energy. In order to remove the radioactive cobalt isotopes from the surface of the structures of the reactor, decontamination solutions can be used. These solutions can contain organic complexing agents, like ethylenediaminetetraacetic acid (EDTA). Thus, cobalt is present in the solutions as a non-ionic species, complexed with EDTA. This creates a challenge since the removal of cobalt-EDTA complexes may not be possible by using conventional methods, like ion exchange. In addition, the waste solutions quite often contain high concentrations of stable metals and only trace concentrations of radioactive cobalt.

Even though the usage of EDTA in the nuclear industry has decreased, vast amounts of EDTA bearing radioactive liquid waste are stored in tanks. The stability of cobalt-EDTA complexes is rather high and efficient oxidation methods are required for the degradation of the complexes. Advanced Oxidation Techniques have proven their usability for the degradation of EDTA and became also the main motivation of this dissertation together with the removal of cobalt by using inorganic sorbent materials.

The dissertation summarizes the usability evaluations of different inorganic sorbent materials for the cobalt uptake in EDTA bearing solutions. A commercial titania based ion exchange material CoTreat® (manufactured by Fortum Power and Heat Oy) was tested in combination with different Advanced Oxidation Techniques including ozonation and ultraviolet (UV) irradiation. When the process was divided into two stages, first the oxidation of EDTA as a pretreatment, and secondly the removal of cobalt by CoTreat®, very good results were achieved. Other sorbent materials under study were synthesized titanium antimonates and antimony oxides. The titanium

antimonates were tested without the oxidation of EDTA and proved their usability to remove cobalt especially in acidic solutions. When the synthesized antimony oxides were studied, it was noticed that UV irradiation had a favourable effect on the cobalt sorption efficiency even in the absence of EDTA in the solution. It was demonstrated that a single-stage process combining the UV oxidation and removal of cobalt can be utilized with antimony oxides. Interfering ions, like calcium or nickel in the solution affected the cobalt sorption efficiency of antimony oxide. However, the obtained results were encouraging and the possibility to use antimony oxide as an efficient sorbent for cobalt from aqueous nuclear waste became clear.

Keywords: cobalt; EDTA; sorption; titania; titanium antimonate; antimony oxide; Advanced Oxidation Techniques; UV-C; competing cations

ACKNOWLEDGEMENTS

The research for this work was conducted in the ion exchange group, Department of Chemistry - Radiochemistry at University of Helsinki. I am grateful for the financial support I obtained from Business Finland (former TEKES), Fortum Foundation and Jenny and Antti Wihuri Foundation. Roy G. Post Foundation is acknowledged for the personal scholarship and for the travel grant that enabled my first participation to the annual Waste Management Symposia.

This work would not have been possible without the help and support of numerous people. I owe my gratitude to my supervisor, the late Risto Harjula, who introduced me to the topic of my thesis with his great enthusiasm towards research. It took a long time to finalize this work and it wouldn't have happened without two important persons, Gareth Law and Nina Huittinen. Gareth, thank you for the encouragement and your help with all the dissertation related procedures. Nina, I find it difficult to find the words to express my gratitude. Thank you.

The pre-examiners of this thesis, Prof. Ulla Lassi and Dr. Nick Evans, are thanked for their comments that helped to improve the quality of the manuscript. Professor Sarah Heath is gratefully acknowledged for accepting the role of the opponent for the public examination.

Eveliina Repo, it was great starting my PhD studies with you and to watch your fast growth as a scientist. Along the way you have always been ready to help, thank you. I want to acknowledge Risto Koivula especially for introducing me the work with radionuclides and Jukka Lehto for stepping in to support my studies when needed. I want to thank Raimo Hyttinen for your expertise and constant willingness to help.

Nina, Mirkka and Miia, you have been walking this path with me right from the beginning. I appreciate your friendship and our empowering discussions. I have had the priviledge to work in the same lab especially with Maria, Ria, Anna-Elina, Sanna K., Valtteri, Elmo, Ilkka, Satu and Airi. Your company filled with endless friendliness and encouragement made even the routine work at

the laboratory feel like fun. I'm also thankfull for all the discussions with Maria, Sinikka, Jenna and Merja, especially while enjoying a nice dinner.

I also want to thank other personnel of the Radiochemistry unit, my office roommate Pirkko, Kerttuli, Maikki, Susanna, Anu, Wenzhong, Junhua, Jussi, Mikko, Janne, Outi, Teija, Taneli…for your kindness and help. I appreciate the support and friendliness of the Inorganic Chemistry unit especially with XRD, thank you Mikko H.

Special thanks go to my superiors at Fortum, Jyrki, Anni and Toni, for the encouragement and for offering me the chance to use office-hours to finalize the thesis.

I want to thank my parents for the care and support. Äiti and Isä, warmest thank you for being there for me and our whole family.

There are also other important persons, friends and close relatives, who might not have contributed to the contents of this thesis but who are making life much more fun and interesting. I am grateful for you for understanding also the deep waters I faced along the way, for sharing your energy even from distance, for the refreshing moments on the walking and jogging trails, for the family dinners, for saying the right words to help me to understand how I can get forward… Thank you all.

Antti, Senni and Timi, you are keeping my life balanced. I want to thank you for everything with all my love.

Hyvinkää, March 2020, *Leena*

CONTENTS

LIST OF ORIGINAL PUBLICATIONS

This thesis is based on the following publications:

I. L. K. Malinen, R. Koivula, R. Harjula, **Removal of radiocobalt from EDTA-complexes using oxidation and selective ion exchange**. *Water Science & Technology* **2009**, 60(4), 1097-1101.

II. L. K. Malinen, R. Koivula, R. Harjula, **Sorption of radiocobalt and its EDTA complex on titanium antimonates**. *Journal of Hazardous Materials* **2009**, 172, 875-879.

III. L. Malinen, R. Koivula, R. Harjula: **Removal of cobalt from aqueous solution containing EDTA under UV-C irradiation by antimony oxide**. *Radiochimica Acta* **2016**, 104(6), 415-422.

IV. L. Malinen, R. Harjula, E. Repo, N. Huittinen, **The effect of UV-C irradiation and EDTA on the uptake of Co^{2+} by antimony oxide in the presence and absence of competing cations Ca^{2+} and Ni^{2+}.** *Under review.*

The publications are referred to in the text by their roman numerals.

Author contributions:

I. All authors planned the research. L. K. Malinen conducted all the experiments and wrote the manuscript. R. Koivula and R. Harjula commented on the manuscript.

II. All authors planned the research. R. Koivula synthesized the materials. L. K. Malinen conducted all the experiments and wrote the manuscript. R. Koivula and R. Harjula commented on the manuscript.

III. All authors planned the research. L. Malinen and R. Koivula synthesized the material. L. Malinen conducted all the experiments, except the surface area and pore size analysis. L. Malinen wrote the manuscript. R. Koivula and R. Harjula commented on the manuscript.

IV. L. Malinen and R. Harjula planned the research. L. Malinen synthesized the material and conducted all the experiments, except the surface area and pore size analysis. E. Repo fitted the sorption isotherm models to the experimental data. L. Malinen and N. Huittinen wrote the manuscript with equal contribution.

ABBREVIATIONS

ALARA	as low as reasonably achievable
AOT	Advanced Oxidation Technique
BET	Brunauer, Emmett and Teller
BWR	boiling water reactor
CoTreat®	commercial titania
Degussa P25	commercial photocatalyst material
DF	decontamination factor
EDTA	ethylenediaminetetraacetic acid
EDX	energy dispersive X-ray spectroscopy
EPRI	Electrical Power Research Institute
FESEM	field emission scanning electron microscope
HP/CORD®	permanganic acid/chemical oxidation reduction decontamination
K_D	sorption distribution coefficient (mL g^{-1} or L kg^{-1})
MDA	minimum detectable activity
NPP	nuclear power plant
PWR	pressurized water reactor
PZC	point of zero charge
SOH	surface hydroxyl site
TiSbA	titanium antimonate, synthesis A
TiSbB	titanium antimonate, synthesis B
UV	ultraviolet
UV-VIS	ultraviolet visible
XRD	X-ray diffraction
XRF	X-ray fluorescence

Note: the list does not include either parameters or standard chemical formulae.

1 INTRODUCTION

1.1 RADIOACTIVE COBALT IN AQUEOUS NUCLEAR WASTE

Cobalt is a transition metal which has 28 characterized radioisotopes. Most of these radioisotopes have half-lifes less than 18 hours. Longer half-lifes belong to the following radioisotopes: ^{60}Co, ^{57}Co, ^{56}Co and ^{58}Co (see Table 1), which can be referred to as the *main radioisotopes of cobalt*. The decay mode for ^{60}Co is beta decay, and for $^{56\text{-}58}$Co electron capture. The decay schemes for ^{60}Co and ^{57}Co are presented in more detail in Figures 1 and 2, respectively.

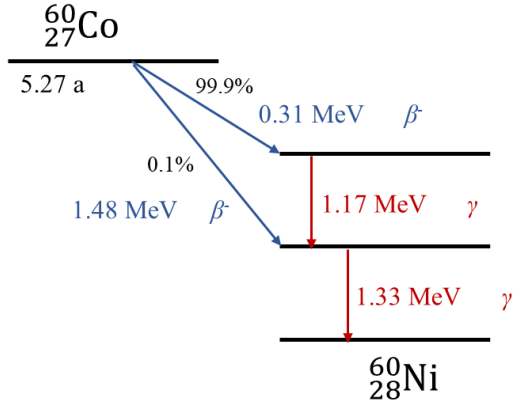

Figure 1 Decay scheme for ^{60}Co (data obtained from Chu et al., 1999).

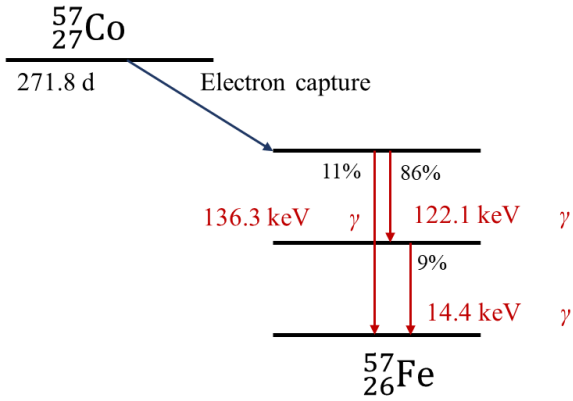

Figure 2 Decay scheme for ^{57}Co (data obtained from Chu et al., 1999).

The gamma decay energies of ^{60}Co are high, 1332 and 1173 keV (Chu et al., 1999), compared to the gamma decay energies of the other main isotopes (Table 1).

Table 1 The gamma decay energies with intensity over 80% of the main radioisotopes of cobalt (Chu et al., 1999).

Radioisotope	E_γ (keV)	I_γ (%)	Decay mode	Half life
^{60}Co	1332 1173	99.99 99.97	β^- β^-	5.27 y
^{57}Co	122	85.60	ε	271.79 d
^{56}Co	846	100	ε+β^+	77.27 d
^{58}Co	810	99.00	ε+β^+	70.86 d

Two of the main isotopes, ^{60}Co and ^{58}Co, can be produced by neutron capture in nuclear power plants (NPPs). Production of ^{60}Co and ^{58}Co emerge through the following reactions:

(1) ^{59}Co(n, γ)^{60}Co,

(2) ^{58}Ni(n, p)^{58}Co,

where ^{59}Co and ^{58}Ni are stable isotopes of cobalt and nickel, respectively. The stable isotopes of cobalt and nickel are present in the structural components of the NPP reactor. Before going to the origin of the neutrons needed for the above reaction, we can take a closer look at the conditions at the NPP reactor. For pressurized water reactors (PWRs) and boiling water reactors (BWRs) the conditions are approximately the following:

Temperatures ≤ 350^{0}C

Pressures ≤ 16 MPa

Intense γ- and neutron irradiation

The conditions cause potentially severe corrosive conditions for the reactor materials (Choppin et al., 2013). Corrosion leads to the release of small amounts of Fe, Cr, Co, and Ni in the cooling circuit. These corrosion products are impurities in the cooling circuit and may exist in ionic, colloidal and

insoluble oxide / mixed oxide forms. The insoluble oxides and mixed oxides are referred to as *crud* and can be defined as the particulates which can can be filtered at ambient temperature by 0.45 μm Millipore membrane (Lin, 2009). Iron is the dominating corrosion product in BWR coolant (concentration can be over 90%), but nickel concentration may be as high as 20% (Lin, 2009). The PWR coolant contains similar concentrations of iron and nickel (Grygar and Zmitko, 2002). Crud can also contain for example copper from the BWR condenser system or boron from the boric acid control system for PWR (Choppin et al., 2013). The concentration of cobalt is generally very low, less than 1% of the total concentration of the corrosion products (Lin, 2009).

Formation of corrosion products in BWR and PWR is affected by the composition of the reactor materials and the cooling water chemistry, thus concentrations of corrosion products may vary in each reactor. In addition, the solubility of each corrosion product plays an important role in their transport behavior in the cooling circuit. As an example of the complexicity of the transport of corrosion products, a block diagram of corrosion product transport in BWR primary cooling system is presented in Figure 3. The terms "inner layer" and "outer layer" used in Figure 3 refer to the possible double layer formation which has been observed for example on fuel cladding surfaces (Lin, 2009). The "inner layer" and "outer layer" can be separated by differencies in their metal oxide composition (Lin, 2009).

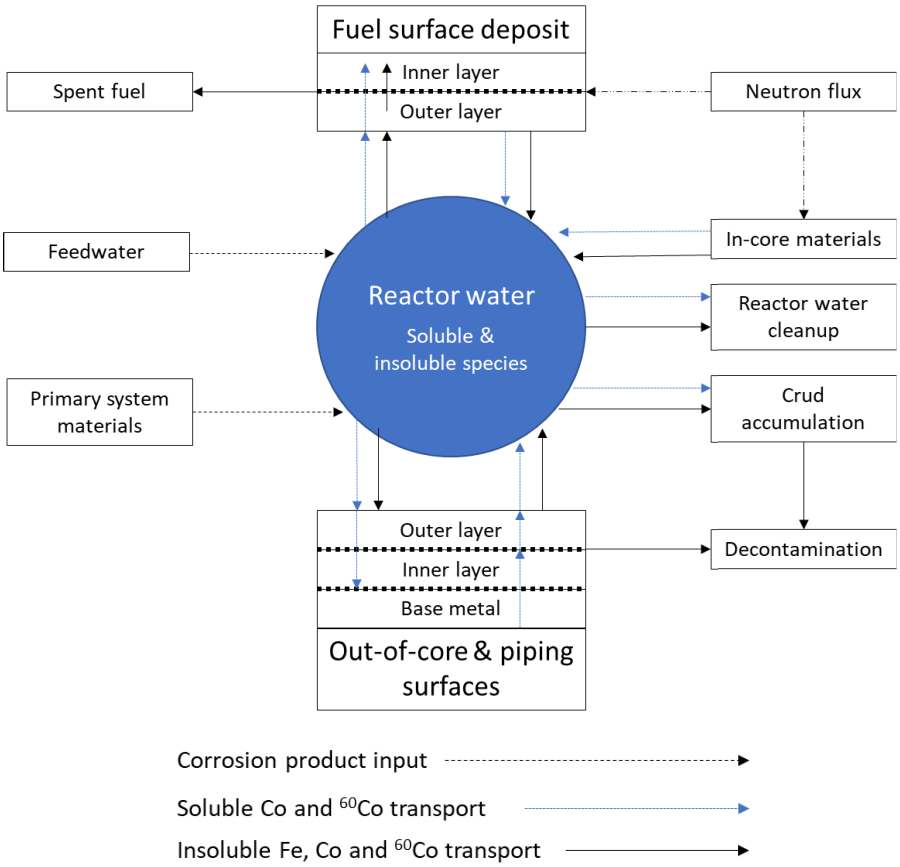

Figure 3 Block diagram of corrosion product transport in BWR primary system (reproduced from Lin, 2009).

The activation of the corrosion products takes place due to the neutron absorption when the products pass the reactor core and results in the formation of ^{60}Co and ^{58}Co, as an example. The contaminated inner surfaces of the reactor cooling circuit or its components in the NPP are a source of γ-radiation background for the plant's personnel. It has been estimated that ^{60}Co causes up to 80% of the radiation exposure to the reactor operating personnel (Varga et al., 2001).

Since minimizing the radiation exposure to plant personnel is one of the main concerns in operating nuclear power plants, a variety of decontamination methods are used in order to decrease the γ-radiation background. These

decontamination methods can be divided in mechanical and chemical/electrochemical methods. The most suitable decontamination technique can be selected based on several criteria, e.g. the decontamination factor (DF, usually defined as DF = initial activity/residual activity), the material compatibility, the waste volume, ALARA (As Low As Reasonably Achievable) requirements and commercial values (Kinnunen, 2008).

Mechanical decontamination is usually applied to single components (e.g. the main coolant pump). One of the mechanical decontamination techniques is ultrasonic cleaning which, for example, EPRI (Electric Power Research Institute) has utilized for the decontamination of fuel rods. In the ultrasonic cleaning technique developed by EPRI, an optimum arrangement of special transducers are used. This results in an ultrasonic energy field, which is able to "see around" the intervening fuel rods in the centre of the fuel assembly. The produced energy field has also relatively uniform intensity throughout the fuel matrix. The process produces only the dislodged deposits as waste (Blok et al., 2002).

Chemical decontamination has been applied to both single component and full system decontamination, whereas electrochemical decontamination is usually applied to components. During chemical decontamination, the decontaminated surfaces are treated with different chemicals which dissolve the contamination and oxide layer from the surfaces of the reactor cooling system. Because the oxides of Fe, Ni, and Cr are practically insoluble in pure neutral water, chelating agents are added to the decontamination solutions (Kinnunen, 2008). One example of the chemical decontamination techniques is HP/CORD® UV where oxalic acid is used as a chelating agent (Stiepani and Bertholdt, 2005). The abbreviation stands for:

HP Permanganic acid
C Chemical
O Oxidation
R Reduction
D Decontamination
UV UltraViolet light

The HP/CORD® UV process is applied as an multi-cycle process. These cycles can be divided in following steps (Stiepani and Bertholdt, 2005):

1. Oxidation using permanganic acid ($HMnO_4$);
2. Reduction of permanganic acid using decontamination chemical;
3. Decontamination;
4. UV-decomposition of decontamination chemicals.

In addition to oxalic acid, also ethylenediaminetetraacetic acid (EDTA) has been used to increase the solubility of the metal oxides of crud during decontamination processes (Nelson, 1981). More recently, the usage of EDTA was reported in context with the chemical cleaning process of PWR steam generator (Fujiwara et al., 2006). It was stated that in some PWRs the corrosion products can deposit and adhere to steam generator components which suppresses heat transfer, however, good cleaning efficiency had been achieved with a process containing EDTA (Fujiwara et al., 2006). The specifics of this organic complexing agent are discussed in more detail in the next chapter.

1.2 ETHYLENEDIAMINETETRAACETIC ACID

Ethylenediaminetetraacetic acid (EDTA) is one of the organic complexing agents used in NPP decontamination methods. As a solid compound, EDTA is usually present as the disodium salt dehydrate (Na_2H_2-EDTA•$2H_2O$) (Bergers et al., 1994). The structure of EDTA is presented in Figure 4.

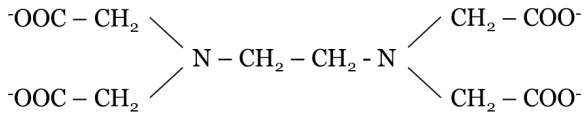

Figure 4 Structure of EDTA (ethylenediaminetetraacetic acid, systematic name N,N' - 1,2-ethanediylbis[N - (carboxymethyl)glycine] disodium salt) (reproduced from Bergers et al., 1994).

EDTA is an amino carboxylic complexing agent that has the ability to form water-soluble 1:1 complexes with di- and trivalent metal ions coordinating the metal ion as is shown in Figure 5.

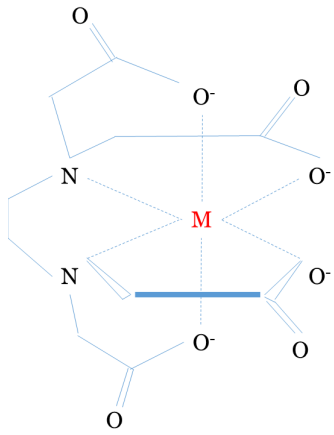

Figure 5 Structure of a metal-EDTA complex.

Compared to other metal-ligand complexes, the ring formation leads to a higher stability of the complexes. EDTA is poorly biodegradable and very heat resistant, implying that formed metal-chelates are very stable and difficult to break apart (Bucheli-Witschel and Egli, 2001). It has been demonstrated, that only Fe(III)-EDTA complexes can be eliminated by photodegradation under environmental conditions in shallow rivers (Kari and Giger, 1995). The main photodegradation products of Fe(III)-EDTA have been reported as carbon dioxide, formaldehyde, N-carboxymethyl-N,N´-ethylenediglycine (ED3A) and N,N'-ethylenediglycine (EDDA-N,N') (Lockhart and Blakeley, 1975, and Metsärinne et al., 2001). Another evaluation of the degradation products of EDTA has been made in a study where EDTA was degraded under UV irradiation in the presence of the commercial photocatalyst Degussa P25 (titania) in pH 3 (Babay et al., 2001). In the research, the possible intermediates of EDTA degradation were named as glycine, ethylenediamine, ammonium, formaldehyde, and formic, iminodiacetic, oxalic, oxamic, glycolic and glyoxylic acids (Babay et al., 2001). The concentrations of produced nitrate, nitrite, and ammonium ion concentrations have been analyzed after TiO_2 mediated photocatalytic oxidation of EDTA in the absence and presence of Fe^{2+}, Cu^{2+}, Zn^{2+}, Ni^{2+} or Co^{2+} ions (Onar and Akdemir, 2007). It was shown that in the presence of Fe^{2+}, Ni^{2+}, and Co^{2+}, the concentration of produced ammonium ion was lower than in the absence of metal ions below pH 7 (Onar

and Akdemir, 2007). The effect of Fe^{2+}, Ni^{2+}, and Co^{2+} on the formation of nitrite and nitrate ions varied indicating that the type of the metal ion present in the photocatalytic reaction medium affects the produced ion concentrations (Onar and Akdemir, 2007). It should be mentioned that some of the degradation products of EDTA (like oxalic acid and ammonia) can form complexes with cobalt and other metals affecting the behavior of metals in the solution. The EDTA degradation processes presented in the dissertation are included in the Advanced Oxidation Techniques, the theory and chemistry of which will be presented in the chapter 1.3 Advanced Oxidation Techniques.

Even though the usage of EDTA in the nuclear industry has been reduced, EDTA bearing liquid wastes generated in earlier years can be found stored in tanks. It has been reported that the 149 radioactive liquid waste tanks at the Hanford Complex in the United States contain 83 tons of EDTA (Samuels et al., 1994). The mobilization of radionuclides from waste disposal sites has been studied in Oak Ridge, Tennessee (Means et al., 1978). The intermediate-level radioactive liquid waste was disposed of in seven different seepage pits and trenches at the Oak Ridge National Laboratory between 1951-1965. The liquid waste contained EDTA which had been used in the decontamination operations at nuclear facilities. It had been studied, that the shale in the Oak Ridge has a high adsorption capacity for cobalt. Thus, Oak Ridge was considered as a suitable area for the disposal of cobalt-containing waste. The mobilization of cobalt should have been negligible. However, in the presence of EDTA, the cobalt adsorption capacity of the shale was drastically reduced and mobilization rate of cobalt was possibly accelerated by several orders of magnitude (Means et al., 1978).

The possible effect of EDTA on the leachability and mobility of radionuclides, including cobalt, needs to be taken into account when evaluating the quality of the radioactive wastes. Thus, the degradation of EDTA can be seen favorable considering the safe and efficient disposal of radioactive waste.

1.3 ADVANCED OXIDATION TECHNIQUES

Advanced Oxidation Techniques (AOTs) can be defined as processes generating sufficient quantity of hydroxyl radicals to affect water purification. The reactivity of the hydroxyl radicals is exploited in oxidation processes which are suitable for the degradation of organic substances, like EDTA (Chitra et al., 2013). Advanced Oxidation Techniques include the following processes (Andreozzi et al. 1999):

- H_2O_2 / Fe^{2+} (Fenton)
- H_2O_2 / Fe^{3+} (Fenton-like)
- H_2O_2 / Fe^{2+} (Fe^{3+}) / UV (Photo assisted Fenton)
- H_2O_2 / Fe^{3+} - Oxalate / UV (Photo assisted Fenton)
- Mn^{2+} / Oxalic acid / Ozone
- TiO_2 / hν / O_2 (Photocatalysis)
- O_3 / H_2O_2
- O_3 / UV
- H_2O_2 / UV

1.3.1 FENTON PROCESSES

One of the widely studied applications of Advanced Oxidation Techniques is the production of hydroxyl radicals by Fenton's reagent which is a combination of hydrogen peroxide and iron(II) (ferrous) salts (Andreozzi et al., 1999):

(3) $$Fe^{2+} + H_2O_2 \rightarrow Fe^{3+} + OH^- + HO^{\bullet}$$

Iron is an abundant and non toxic element and hydrogen peroxide is easy to handle and environmentally safe chemical, which makes this oxidative system attractive for waste water treatment (Andreozzi et al., 1999). At a pH value of 2.7 - 2.8, Fe^{3+} can be reduced to Fe^{2+} producing hydroxyl radicals (Andreozzi et al., 1999):

(4) $$Fe^{3+} + H_2O_2 \leftrightarrow H^+ + FeOOH^{2+}$$

(5) $$FeOOH^{2+} \rightarrow HO_2^{\bullet} + Fe^{2+}$$

This process is called a *Fenton-like* process and in these conditions, iron can be considered as a catalyst.

1.3.2 PHOTOASSISTED FENTON PROCESSES

It is possible to accelerate the rate of degradation of organic substances with Fenton and Fenton like reagents by irradiation with UV-VIS light (Andreozzi et al., 1999). When the UV-VIS light irradiation is at wavelength values higher than 300 nm, the photolysis of Fe^{3+} complexes allows Fe^{2+} regeneration:

(6) $$Fe(OH)^{2+} \xrightarrow{h\nu} Fe^{2+} + HO^{\bullet}$$

Due to the presence of H_2O_2, the process continues as was presented in reaction (3).

An improvement of photoassisted Fenton processes is the utilization of ferrioxalate in the process (Safarzadeh-Amiri et al., 1996):

(7) $$[Fe^{III}(C_2O_4)_3]^{3-} + h\nu \rightarrow [Fe^{II}(C_2O_4)_2]^{2-} + C_2O_4^{\bullet-}$$

(8) $$C_2O_4^{\bullet-} + [Fe^{III}(C_2O_4)_3]^{3-} \rightarrow [Fe^{II}(C_2O_4)_2]^{2-} + C_2O_4^{2-} + 2CO_2$$

(9) $$C_2O_4^{\bullet-} + O_2 \rightarrow O_2^{\bullet-} + 2CO_2$$

The ferrous ions, Fe^{2+}, formed in the process can be free or complexed with oxalate. When hydrogen peroxide is added to the solution, the ferrous ions react with hydrogen peroxide generating hydroxyl radicals through reaction (3). Thus, the photolysis of ferrioxalate in the presence of hydrogen peroxide provides a continuous source of Fenton's reagent (Zepp et al., 1992). One benefit of using ferrioxalate originates from its ability to absorb UV light over a broad range of wavelengths, 250 - 500 nm (Safarzadeh-Amiri et al., 1997).

1.3.3 UTILIZATION OF OZONE

Hydroxyl radicals can also be generated in the presence of short wavelength UV irradiation from hydrogen peroxide in the presence of ozone. Ozone has a strong UV absorbance especially at around 254 nm wavelength. Absorption of UV radiation leads to the decomposition of aqueous ozone and can be presented with following equations (Bains et al., 2003):

(10) $O_3 + UV\ irradiation \rightarrow O_2 + O^*\ (an\ excited\ oxygen\ atom)$

(11) $O^* + H_2O \rightarrow 2\,HO^\bullet$

(12) $O^* + H_2O \rightarrow H_2O_2 + UV\ irradiation \rightarrow 2\,HO^\bullet$

Ozone has a short life time in alkaline solutions. One possible route for the decomposition of ozone in aqueous solution developes through the formation of OH radicals, OH^- ions acting as the initiator (Gardoni et al., 2012):

(13) $HO^- + O_3 \rightarrow O_2 + HO_2^-, where\ HO_2^- \overset{H+}{\leftrightarrow} H_2O_2$

(14) $HO_2^- + O_3 \rightarrow HO_2^\bullet + O_3^{\bullet-}$

(15) $HO_2^\bullet \leftrightarrow H^+ + O_2^{\bullet-}$

(16) $O_2^{\bullet-} + O_3 \rightarrow O_2 + O_3^{\bullet-}$

(17) $O_3^{\bullet-} + H^+ \rightarrow HO_3^\bullet$

(18) $HO_3^\bullet \rightarrow OH^\bullet + O_2$

(19) $OH^\bullet + O_3^{\bullet-} \rightarrow OH^- + O_3$

Hydrogen peroxide is formed during the ozone decomposition in aqueous solution. However, the addition of hydrogen peroxide to the ozone containing solution will enhance the ozone decomposition by the formation of hydroxyl radicals. The efficiency of the process is highly affected by the solution pH since the concentration of the conjugate base, HO_2^-, is dependent on pH. Since

HO_2^- is an active species in the ozone decomposition process, its concentration affects the decomposition efficiency (Andreozzi et al., 1999).

One option to enhance ozone decomposition is to use the Mn^{2+}/oxalic acid system to produce hydroxyl radicals. In this process Mn^{2+} catalyses the ozonation of oxalic acid at pH above 4. Mn(III)-dioxalate and Mn(III)-trioxalate are formed and it has been presumed that the process proceeds through the formation of hydroxyl radicals (Andreozzi et al., 1992):

(20) $$Mn(III)(AO^{2-})_n + O_3 + H^+ \rightarrow Mn(II) + (n-1)(AO^{2-}) + 2CO_2 + O_2 + HO^{\bullet}$$

1.3.4 H_2O_2/UV AND O_3/UV PROCESSES

It is possible to produce hydroxyl radicals by combining UV light with hydrogen peroxide or ozone. In hydrogen peroxide photolysis (H_2O_2/UV), the solution containing organic species and hydrogen peroxide is irradiated with UV light having wavelengths smaller than 280 nm. Homolytic cleavage of hydrogen peroxide occurs in these conditions (Anreozzi et al., 1999):

(21) $$H_2O_2 \xrightarrow{h\nu} 2\,HO^{\bullet}$$

Hydrogen peroxide itself is attacked by hydroxyl radicals:

(22) $$2(H_2O_2 + HO^{\bullet}) \rightarrow H_2O + HO_2^{\bullet}$$

(23) $$HO_2^{\bullet} \rightarrow H_2O_2 + O_2$$

In the process where ozone and UV light are combined (O_3/UV), aqueous solution saturated with ozone is irradiated with UV light of 254 nm in a suitable reactor. It has been reported that the principal active species in photolytic ozonation is the hydroxyl radical. In addition, the photolysis of aqueous ozone directly yields hydrogen peroxide. Hydrogen peroxide participates in secondary reactions with ozone to produce hydroxyl radicals. The main two routes can be simplified as follows (Peyton and Glaze, 1988):

(24) $$O_3 + H_2O \xrightarrow{hv} O_2 + H_2O_2$$

(25) $$O_3 + H_2O_2 \xrightarrow{hv} O_2 + 2\,HO^{\bullet}$$

1.3.5 PHOTOCATALYSIS

Titania is one of the most efficient materials used to catalyze the photodegradation of organic materials under UV irradiation. According to general acceptance, the anatase phase of titania exhibits higher photocatalytic activity compared to the rutile phase of titania (Luttrell *et al.*, 2014). However, the most commonly used titania photocatalyst, Degussa P25, is a mixture of both, anatase and rutile phases. One of the explanations for this enhanced photocatalytic effectiveness of the mixed phased Degussa P25 has been divided into three factors (Hurum *et al.*, 2003):

1) Useful range of photoactivity is widened into visible region due to the smaller band gap of rutile phase.
2) Charge separation is stabilized by electron transfer from rutile to anatase slowing down recombination.
3) The electron transfer is facilitated by the small size of the rutile crystallites. Thus, particle size and the interface between the rutile / anatase interface are crucial for the process.

Titania is a semiconductor which produces electron-hole pairs, $e^- + h^+$, under UV irradiation at wavelengths of 390 nm or less (Madden et al., 1996). The photocatalytic process with TiO_2 is initiated by the excitation of TiO_2 by UV light (Fujishima et al., 2000):

(26) $$TiO_2 + hv \rightarrow e^- + h^+$$

The formed electrons can reduce some metals and dissolved oxygen forming the superoxide radical ion $O_2^{\bullet-}$. The remaining holes located at the TiO_2 valence band can migrate to the surface of the catalyst and produce hydroxyl radicals by oxidizing water or hydroxide, HO^- (Andreozzi et al., 1999):

(27) $TiO_2(h^+) + H_2O_{ad} \rightarrow TiO_2 + HO^{\bullet}_{ad} + H^+$

(28) $TiO_2(h^+) + HO^-_{ad} \rightarrow TiO_2 + HO^{\bullet}_{ad}$

Direct oxidation of an adsorbed species on the surface of the photocatalyst is also possible by direct hole oxidation (Andreozzi et al., 1999):

(29) $TiO_2(h^+) + RX_{ad} \rightarrow TiO_2 + RX^{\bullet+}_{ad}$

1.4 SELECTED SORBENT MATERIALS

The ion exchange properties of various metal oxides and hydrous metal oxides have been studied. Many of these studied materials are sparingly soluble solid materials which have an excess positive or negative charge localized in specific locations in the functional groups or framework structure of the material. The materials have an ability to change a charged ion from a solution to an equivalent ionic amount of other ions from their surface (Helfferich, 1995). Inorganic sorbent materials are generally stable to ionizing radiation and to relatively high temperatures which makes them suitable for use in nuclear waste processing (Clearfield, 2000). Quite often the aqueous nuclear waste contains only trace amounts of radionuclides and high concentrations of stable metal ions. It has been reported that the concentration of ^{60}Co in a floor drain water at the Loviisa nuclear power plant in Finland is $9.5 \cdot 10^{-13}$ mol L^{-1}, whilst the concentrations of various stable ions or compounds are comparatively high: $1.6 \cdot 10^{-3}$ mol L^{-1} Na^+, $0.2 \cdot 10^{-3}$ mol L^{-1} K^+, $0.02 \cdot 10^{-3}$ mol L^{-1} Ca^{2+} and $2.6 \cdot 10^{-3}$ mol L^{-1} H_3BO_3 (Harjula et al., 1999 *b*). The removal of cobalt from the liquid waste can be influenced by the macro-elements, especially the divalent cation Ca^{2+}. Also other chemically similar transition metals present in the liquid waste in much lower concentrations, may compete for the sorption sites on the solid material. Thus, high selectivity of the sorption material is required for efficient removal of radionuclides.

It has been reported that when hydrous metal oxides were heated, the ion exchange capacity of the material was decreased (Granados et al., 2006). Since heating eliminates water from the metal oxide, it was concluded that the water contained in the particles of the metal oxide is responsible for the ion exchange of the hydrous metal oxides, as presented in Figure 6. This ion exchange reaction could be written as follows (Granados et al., 2006) for the sorption of cobalt:

(30) $$MO_x nH_2O + mCo^{2+} \leftrightarrow MO_x\big((n-m)H_2O mCoO\big) + 2mH^+$$

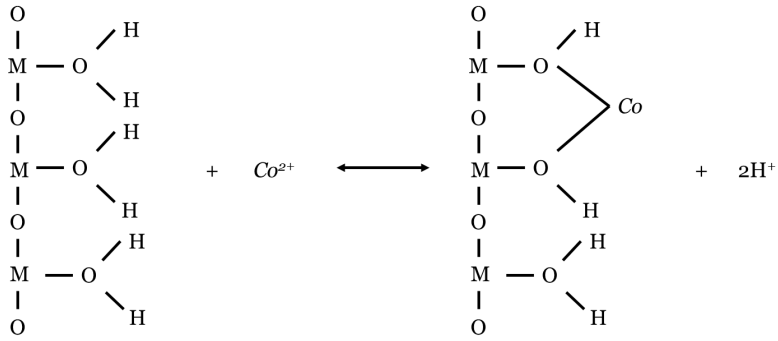

Figure 6 Ion exchange of hydrous oxides and cobalt in solution (reproduced from Granados et al., 2006).

In this chapter, the sorbent materials selected for the dissertation are briefly introduced. Also, an explanation is given for the grounds of choosing the materials for the study.

1.4.1 TITANIA

The hydrous form of titania can be used as an ion exchange material for radionuclides such as strontium and cobalt (Abe, 1982). Titania exists as two main polymorphs, anatase and rutile (Hanaor and Sorrell, 2011). The bulk structure of rutile and anatase phases of titania are presented in Figure 7. Both of these titania types, rutile and anatase, exist also as hydrous oxides and are insoluble in the pH range from 1 to 12 (Abe, 1982).

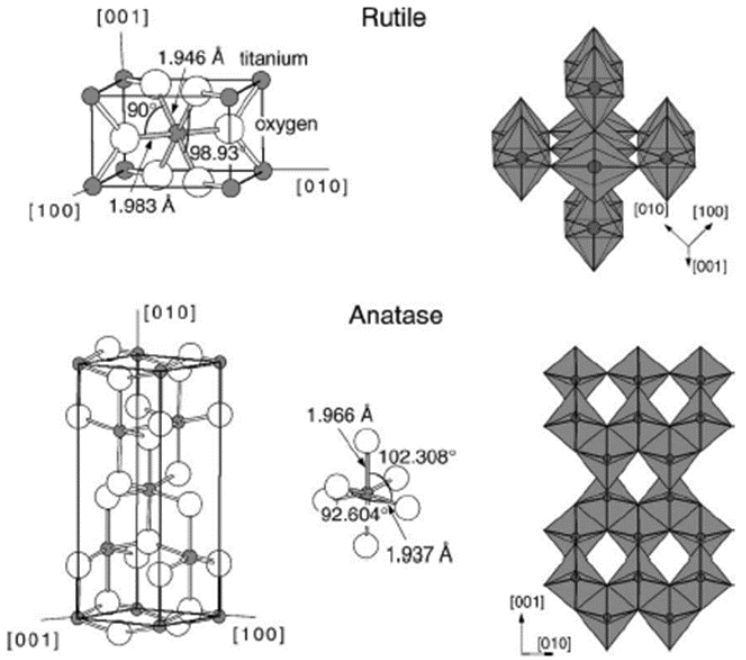

Figure 7 Bulk structures of rutile and anatase. The tetragonal bulk unit cell of rutile has the dimensions, a = b = 4.587 Å, c = 2.953 Å, and the one of anatase a = b = 3.782 Å, c = 9.502 Å. In both structure, slightly distorted octahedra are the basic building units. The bond lengths and angles of the octahedrally coordinated Ti atoms are indicated and the stacking of the octahedral in both structure is shown on the right. (Reprinted with the permission of Elsevier from Diebold, 2003.)

One of the commercially available sorbent materials based on titania is CoTreat® (Fortum Power and Heat Oy, Finland) which is highly selective for ^{58,60}Co and other corrosion product nuclides (^{54}Mn, ^{59}Fe, ^{65}Zn and ^{63}Ni) (Harjula et al., 1999 *a*). It has been reported that CoTreat® is supplied in mixed Na^+/H^+ -form and that the material is poorly crystalline or microcrystalline (Harjula et al., 2010). Processing capacities in the range of 50,000 – 500,000 L kg^{-1} should be obtainable for the removal of ^{58,60}Co using CoTreat® (Harjula et al., 1999 *a*). Controlling the pH of the water to be treated is crucial for achieving high removal efficiencies since CoTreat® has its optimum operating pH area between pH 5-7.

CoTreat® was selected as one of the sorbent materials for cobalt in this dissertation since its sorption efficiency in accordance with advanced oxidation techniques has not been studied before. As was mentioned, the

sorbent material has proven efficiency for the removal of cobalt when cobalt is in free, ionic form. This was seen as a good basis for the research on the required pretreatment methods for cobalt removal in the presence of EDTA.

1.4.2 TITANIUM ANTIMONATES

One of the driving forces to study the ion exchange properties of titanium antimonates has been the need for an acidic ion exchange material which could remove strontium from acidic solutions in the presence of calcium (Möller et al., 2003). It has been concluded that the ion exchangers calcium tolerance in strontium exchange could be derived by using titania and the acidity of the material could be increased by using antimony (Karhu et al., 2000). The most suitable molar ratio of Ti and Sb in titanium antimonate has been studied e.g. for the removal of alkali metal ions from nitric acid solutions. The results indicated that a titanium antimonate material with Ti:Sb ratio of 1.56 has a larger number of stronger acid sites available for ion exchange than that of Ti:Sb ratio 3.7 (Abe et al., 1985). Thus, the material with Ti:Sb ratio of 1.56 exhibited higher ion exchange efficiency. The rather odd molar ratios of Ti and Sb in the materials originate from the molar ratios used in the synthesis of the materials. When the Ti:Sb ratio of 1.5 was used in the synthesis solution, the molar ratio in the material was 1.56. Respectively, when the Ti:Sb ratio of 3.0 was used in the synthesis, the molar ratio of the material was 3.7. (Abe et al., 1985)

A selectivity series of titanium antimonates with increasing ion exchange property follows the order $Na^+ < K^+ < Rb^+ < Li^+ < Cs^+$ for alkali-metal ions in hydrochlorid acid media (Abe and Tsuji, 1983) and $Mn^{2+} < Ni^{2+} < Cd^{2+} < Zn^{2+} < Co^{2+} < Cu^{2+} < Fe^{2+}$ for divalent transition metal ions in nitric acid media (Chitrakar and Abe, 1986). The structure of titanium antimonates has been described to consist of a titanate ´backbone´and -OSbH groups which are evenly distributed onto the titanate matrix (Abe et al., 1985).

Titanium antimonates are interesting sorption materials due to the acidity of the sorbents. In addition, there was no information available about the

cobalt sorption efficiency of titanium antimonates in the presence of EDTA. Thus, the materials were selected to be studied in this dissertation.

1.4.3 ANTIMONY OXIDES

One of the first studies revealing the usability of antimony oxides as ion exchange material was published in 1968 discussing the cation-exchange behaviour and surface functionality of three different antimonic acids, amorphous, glassy and crystalline (Abe and Ito, 1968). The materials were heated in order to see the effect of the loss of water to the ion exchange capacity. The loss of chemically bonded water caused decrease in the ion exchange capacity of the amorphous and glassy antimonic acids. Heating of the crystalline acid (within 200^{0}C) didn't have effect on the ion exchange capacity. It was concluded that the loss of the interstitial (free) water doesn't have an effect on the ion exchange capacity of the material and no drastic change occurs on the surface structure of the crystal when heated up to 200^{0}C. (Abe and Ito, 1968). An estimation of the surface structure of amorphous and glassy antimonic oxide is presented in Figure 8, and that of crystalline antimony oxide in Figure 9.

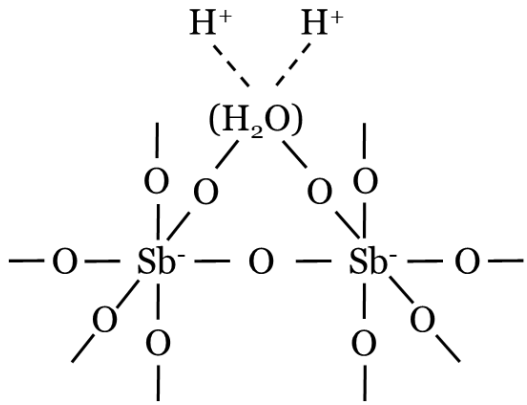

Figure 8 The surface structure of amorphous and glassy antimonic oxide, $Sb_2O_5 \cdot nH_2O$ resembling the pyrochlore form (reproduced from Abe and Ito, 1968).

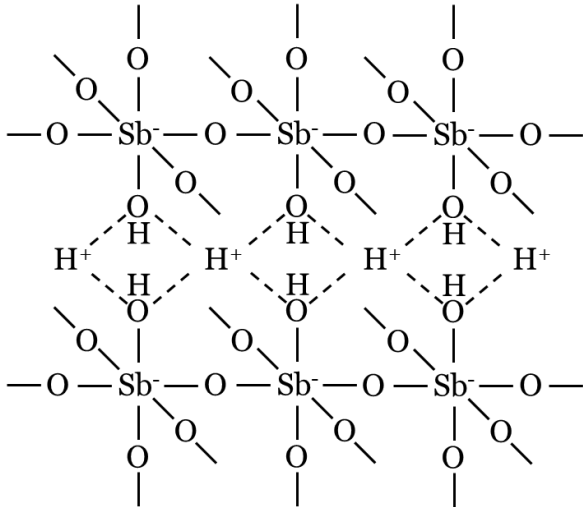

Figure 9 Structure of crystalline antimony oxide, $H_2Sb_2O_5(OH)_2$ (reproduced from Abe and Ito, 1968).

The composition of the pyrochlore form antimony oxide, $Sb_2O_5 \bullet nH_2O$, has been reported to correspond to n = 3 or 4 (Zouad et al., 1992). The pyrochlore 'sceleton' consists of corner sharing ($SbO_{6/2}$) octahedral carrying excess negative charge and two types of protons (protons in hydronium ion, H_3O^+, groups and protons bonded to the framework oxygen) are available for ion exchange (Zouad et al., 1992). The selectivity series of crystalline antimony oxide follows the series $Ni^{2+} < Co^{2+} < Zn^{2+} < Cu^{2+} < Mn^{2+} < Cd^{2+}$ in nitric acid solution (Abe and Sudoh, 1980).

Antimony oxides were selected as sorbent materials in this dissertation in order to deepen the knowledge on cobalt sorption properties of these acidic sorbent materials. No information was available related to the removal of cobalt in the presence of EDTA using antimony oxides. In addition, the effect of UV irradiation on the cobalt sorption efficiency of the sorption materials has not been presented elsewhere.

2 AIM OF THE STUDY

The overarching aim of the thesis is to develop methodologies for cobalt removal from aqueous nuclear waste that contains complexing agents, especially EDTA. The first aim of the thesis is to evaluate the benefits of a two-stage treatment process, where the cobalt-EDTA complexes are first oxidized using Advanced Oxidation Techniques, this is then followed by the removal of cobalt using the commercial titania, CoTreat®. Aim 2 is to improve on this two-stage process, ultimately targeting development of a sorbent material that can be utilized for the selective sorption of cobalt in the presence of EDTA without any additional chemicals. Utilization of a single-stage process offers a more efficient treatment process from the perspective of industrial scale water purification. The development of the sorbent material to meet aim 2 is guided by the sorption performance of CoTreat®.

Reflecting the above aims, the dissertation attempts to address the following research objective:

I) Evaluate the efficiency of the commercial titania, CoTreat®, for the removal of cobalt in a single- and two-stage treatment process.

II) For the two-stage treatment process, evaluate the suitability of different Advanced Oxidation Techniques that can be used in combination with CoTreat®.

III) Utilize the results from (I) and (II) to develop the sorbent material further and evaluate the suitability of the developed sorbent material in a single-stage Co-removal process using UV irradiation as an oxidation method.

IV) Develop the sorbent material synthesis to be done with less harmful chemicals. Utilize the single-stage process from (III) and evaluate the effect of nickel or calcium ions on the sorption.

3 EXPERIMENTAL

3.1 MATERIALS SYNTHESIS

The only commercial sorbent material chosen for this study was the titania material CoTreat® (**article I**), and it was used as received. Other materials, titanium antimonates (**article II**) and antimony oxides (**article III** and **IV**) were synthesized in the laboratory. All synthesized materials were used in powder form with particle size distribution between 100 and 200 mesh (149 - 74 μm).

3.1.1 TITANIUM ANTIMONATES

Titanium antimonates were synthesized by modification (Karhu et al., 2000) of a known method (Abe et al., 1985 and Abe and Tsuji, 1983). Reagents used were 99% titanium tetrachloride and 98% antimony pentachloride.

First, to prepare the material called TiSbA, 4 mL of a mixture of titanium tetrachloride (2.25 mL) and antimony pentachloride (1.75 mL) with a molar ratio of 1.5 was prehydrolyzed with an equal volume (4 mL) of distilled water. The reaction with water is violent, thus extra caution was taken for the preparative work. The synthesis vessel (beaker, volume 2 L) was placed in a safety vessel (plastic bucket, volume 10 L) in order to prevent possible spills from spreading in the fume hood. Distilled water (496 mL) was added mixing the synthesis mixture by using a propeller stirrer. After the addition of water, mixing continued for 30 minutes. The white precipitate formed was allowed to stay in the mother liquor at 60°C overnight. Then the synthesis mixture was centrifuged and the supernatant was removed using suction. The white precipitate was washed by adding distilled water (~500 mL) and mixing the precipitate with the added water for 15 minutes. The mixture was allowed to settle for one hour before removing the supernatant. Washing was repeated until the pH of the wash solution was about 2. Supernatant was removed by suction before drying the precipitate at 110°C overnight.

When synthesizing the material called TiSbB, 10 ml of a mixture of titanium tetrachloride (5.65 mL) and antimony pentachloride (4.35 mL) with a molar ratio of 1.5 was prehydrolyzed with an equal volume (10 mL) of distilled water. The reaction with water is violent, thus extra caution was taken for the preparative work, as was described above for the synthesis of the material TiSbA. After the prehydrolyzation, 6 M sodium hydroxide (240 mL) was added mixing the synthesis mixture by using a propeller stirrer. After the addition of sodium hydroxide, mixing continued for 30 minutes. The white precipitate formed was allowed to stay in the mother liquor at 60°C overnight. Washing was done following the same procedure as described above for the material TiSbA with the exception that washing was continued until the pH of the wash solution was about 11.5. Supernatant was removed by suction before drying the precipitate at 110°C overnight.

3.1.2 ANTIMONY OXIDES

In **article III**, antimony pentachloride (25 mL) was dissolved in 6 mol L^{-1} hydrochloric acid (150 mL). The reaction is rather violent, thus extra caution was taken for the preparative work. The synthesis vessel (beaker, volume 2 L) was placed in a safety vessel (plastic bucket, volume 10 L) in order to prevent possible spills from spreading in the fume hood. To the resulting solution was slowly added aqueous ammonia (25% NH_3 / 75% H_2O) maintaining the temperature of the reaction mixture below 70°C. Continuous mixing of the solution was done by using a propeller stirrer. The reaction with ammonia is also violent, thus, it was important to proceed with caution. Ammonia was added until the pH of the mixture was about 2. The addition required ten minutes. The mixing was continued for 30 minutes. The reaction mixture was allowed to stand over night in order to allow the precipitate to settle. The supernatant was removed from above the resulting precipitate by suction. The white precipitate was washed by adding distilled water (~500 mL) and mixing the precipitate with the added water for 15 minutes. The mixture was allowed to settle for one hour before removing the supernatant. Washing was repeated three times. After the third time, the mixture was allowed to settle over night.

Supernatant was removed by suction before drying the precipitate at 110°C overnight.

In **article IV**, antimony oxide was synthesized from potassium hexahydroxoantimonate instead of antimony pentachloride. Potassium hexahydroxoantimonate is a less harmful chemical than antimony pentachloride (corrosive) and is therefore more suitable for larger scale production. The synthesis of antimony oxide was performed by modifying a previously reported synthesis (Khan and Alam, 2004). Instead of keeping the reaction mixture at room temperature overnight, $KSb(OH)_6$ (0.1 mol) and 5.8 M hydrochlorid acid (1 L) were mixed using magnetic stirring and heated to 60°C. Mixing was continued for 30 minutes to dissolve $KSb(OH)_6$ in the acid. To the resulting solution was slowly added aqueous ammonia (25% NH_3 / 75% H_2O) maintaining the temperature of the reaction mixture below 70°C. The solution was continuously mixed. Ammonia was added until the reaction mixture pH rose to 2.0. The addition required 20 minutes. The mixing was continued for 30 minutes. The reaction mixture was allowed to stand for one hour in order to allow the precipitate to settle. The supernatant was removed from above the resulting precipitate by suction. The white precipitate was washed by adding distilled water (~1 L) and mixing the precipitate with the added water for 15 minutes. The mixture was allowed to settle for one hour before removing the supernatant. Washing was repeated three times. After the third time, the mixture was allowed to settle over night. Supernatant was removed by suction before allowing the precipitate to dry at room temperature.

3.2 CHARACTERISATIONS

The identification of the crystal phase of the synthesized materials was determined by powder X-ray diffraction (XRD) using a Panalytical X'pert Pro MDP X-ray diffraction system and X'pert High Score Plus software. The generator was operated at 40 kV and 40 mA. The powder samples were poured on the sample holder and the surface was cautiously equalized using a spattle.

The zeta potential of the synthesized materials was measured with a Malvern Zetasizer Nano ZS which uses Laser Doppler Micro-electrophoresis and patented M3-PALS (Phase Analysis Light Scattering) to measure the zeta potential. The zeta potential is an electrokinetic potential at the boundary of the so called hydrodynamic slip plane of the solid material and bulk solution. The slip plane is located at a specified distance from the surface of the solid material. The distance is specified according to the hydrodynamically stagnant layer, which is a very thin layer of fluid that adheres to the surface of a charged solid surface. Based on the zeta potential analyses, it is possible to define the point of zero charge (PZC) of the solid material. The point of zero charge is the point at a specified pH value, where the zeta potential approaches zero. (Delgado et al., 2005) E.g. in the pH area, where the zeta potential is negative, the solid material can adsorb only cationic ions on its surface. The samples for the zeta potential analyses where prepared by equilibrating the solid material and 0.01 mol L^{-1} $NaNO_3$ solution (pH adjusted with 0.1 mol L^{-1} HNO_3 or 0.1 mol L^{-1} NaOH as necessary) for three (**article III**) or four days (**article II and IV**) using constant rotary mixing (50 rpm) before filtering the sample solution with a 10 μm Acrodisc PSF filter (PALL Life Sciences). The Malvern Zetasizer Nano ZS is designed to measure 5 nm to 10 μm particles, thus it was decided to use the 10 μm filtering as sample pretreatment.

The surface morphology of the synthesized materials were analyzed using a Hitachi S-4800 field emission scanning electron microscope (FESEM). The powder samples were stick on a double sided carbon tape on an aluminium sample holder, and coated with carbon via sputtering to improve surface conductivity. An Oxford INCA 350 microanalysis system connected to the FESEM was used to measure the energy dispersive X-ray spectroscopy (EDX) spectra in order to identify the elements present in the materials TiSbA and TiSbB (**article II**).

BET (Brunauer, Emmett and Teller) surface area and total pore volume of the synthesized materials were determined by nitrogen adsorption at 77 K using Autosorb-1-C surface area and pore size analyzer (Quantachrome, The UK) which utilizes a dedicated transducer monitoring continuously the

saturation pressure of the cryogenic bath. Prior to the analyses, the samples were degassed in vacuum.

3.3 SEPARATION STUDIES

In this dissertation the term sorption is used to describe every type of capture of a species from the solution on the surface of the sorbent materials. Thus, the term sorption does not include absorption. Sorption can be classified as physical sorption, chemical sorption or electrostatic sorption depending on the type of bonding involved. In physical sorption the adsorbate is held to the surface by van der Waals forces and no exchange of electrons is observed. In chemical sorption a strong interaction, including hydrogen bonding and covalent and ionic bond formation occurs between the adsorbate and the solid surface. Thus, an exchange of electrons between the specific surface sites and solute molecules is involved in the sorption process (Inglezakis and Poulopoulos, 2006).

Electrostatic sorption is commonly classified as ion exchange. It involves Coulomb attractive forces between ions and charged surface sites of the sorbent. Ion exchange is a stoichiometric process where an ion from the solution exchanges places with an ion of the same sign bound to the surface of a solid material (Helfferich, 1995).

An ion exchange process, at its simplest, occurs as a binary ion exchange reaction between ion A and ion B and can be written as (Harjula et al., 2010):

$$z_B A^{z_A} + z_A \bar{B}^{z_B} \leftrightarrow z_A B^{z_B} + z_B \bar{A}^{z_A} \quad (31)$$

where z_A and z_B are the charges of ions A and B, respectively; A and B are the ions in the solution and $\bar{A}$ and $\bar{B}$ are the ions of the ion exchange material. In this dissertation, an ion exchange isotherm is presented as the equivalent ionic fraction of the ion being sorbed, $\bar{A}$, in the exchanger as a function of its equivalent ionic fraction, A, in the solution while other variables (for example temperature) are kept constant. It should also be noted that only carrier free cobalt tracer is used in this study. If the ion exchanger has no preference for A or B, a linear ion exchange isotherm would be formed because the ionic

fractions would remain the same in the ion exchanger and in the solution (Figure 10, dotted line) (Inglezakis and Poulopoulos, 2006). The isotherm is negatively curved if ion *A* is preferred and positively curved if ion B is preferred. Thus, selectivity necessitates a nonlinear isotherm, which is shown in Figure 10 as a curved, solid line for an ion exchanger which has selectivity towards cobalt.

The equilibrium selectivity of the binary ion exchange reaction can be defined by the selectivity coefficient, $K_{A\text{-}B}$ (Helfferich, 1995):

(32) $$K_{A-B} = \frac{\bar{C}_A^{z_B} C_B^{z_A}}{\bar{C}_B^{z_A} C_A^{z_B}}$$

where $\bar{C}$ represents concentrations of the ions in the exchanger and C those in solution.

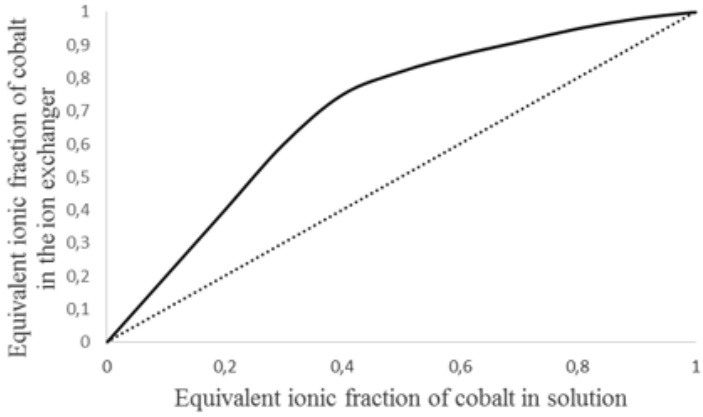

Figure 10 Ion exchange isotherm (solid line) of an ion exchanger with selectivity towards cobalt and an ion exchanger (dotted line) with no preference for either ion (reproduced from Helfferich, 1995).

In this dissertation, the efficiency of the sorption process is presented using the distribution coefficient (K_D, L kg^{-1} or mL g^{-1}), which illustrates the distribution of the solute between the solution and the sorbent material at a certain time:

(33) $$K_D = \frac{q_e}{C_e} = \frac{concentration\ in\ sorbent}{concentration\ in\ solution} = \frac{(R_i - R_{ct})}{R_{ct}} \times \frac{V}{m}$$

where q_e (mol kg^{-1} or mmol g^{-1}) is the experimental cobalt uptake of the sorbent material and C_e (mol L^{-1}) is the cobalt concentration in the solution. R_i (cpm) and R_{ct} (cpm) are the initial count rate of ^{57}Co in the solution and the respective count rate at a certain time, respectively, and are used to represent cobalt concentrations. The so called batch factor, $V\,m^{-1}$ (L kg^{-1}), is the solution volume to sorbent mass ratio and was kept constant (500 L kg^{-1}) in all the experiments in the dissertation. At the time of the experiments of this dissertation, distribution coefficient, K_D, was used in the associated scientific community to describe the sorption efficiency even though the sorption mechanism, or the speciation of cobalt was not known in detail. Instead of K_D, its thermodynamic counterpart, R_D, could have been used. However, the sorption coefficient, R_D, is not utilized in this dissertation.

The sorption efficiency of the sorbent can also be presented as a percentage value:

$$S_{eff} = \left(1 - \frac{C_e}{C_i}\right) \times 100(\%) \tag{34}$$

where C_i is the initial concentration of cobalt in the solution (mol L^{-1}).

The uptake of cobalt in the solid material, q_e, is calculated as follows:

$$q_e = (C_i - C_e) \times \frac{V}{m} \tag{35}$$

The uncertainty of the results was estimated using the propagation of uncertainty:

$$\Delta f = \Delta f(x_1, x_2, \dots, x_n, \Delta x_1, \Delta x_2, \dots, \Delta x_n) = \sqrt{\sum_{i=1}^{n} \left(\frac{\partial f}{\partial x_i} \Delta x_i\right)^2} \tag{36}$$

where Δf is the estimated total uncertainty of f derived from the partial derivate of f with respect to each of the variables $x1, x2, \dots, xn$.

For example, the uncertainty in the K_D value arises from uncertainties in the radioactivity measurements of R_i and R_{ct} and the deviations in V and m. The uncertainty is larger in cases when the K_D value is very high, because the

measured activity then approaches the background level. The estimated total uncertainty of K_D, is calculated as follows:

$$\Delta K_D = \sqrt{\left(\frac{\partial K_D}{\partial R_i}\Delta R_i\right)^2 + \left(\frac{\partial K_D}{\partial R_{ct}}\Delta R_{ct}\right)^2 + \left(\frac{\partial K_D}{\partial V}\Delta V\right)^2 + \left(\frac{\partial K_D}{\partial m}\Delta m\right)^2} = \tag{37}$$

$$\sqrt{\left(\frac{1}{R_{ct}}\Delta R_i \frac{V}{m}\right)^2 + \left(-\frac{R_i}{R_{ct}^2}\Delta R_{ct} \frac{V}{m}\right)^2 + \left(\left(\frac{R_i}{R_{ct}} - 1\right)\frac{\Delta V}{m}\right)^2 + \left(\left(\frac{R_i}{R_{ct}} - 1\right)\left(-\frac{V}{m^2}\Delta m\right)\right)^2}$$

The deviations of V and m have been estimated as 2% and 2.5% respectively taking into account the regularly conducted calibration of the automatic pipettes and scale.

3.3.1 BATCH EXPERIMENTS

The cobalt sorption properties of the synthesized materials in **article II-IV** and CoTreat® in **article I** were examined using ^{57}Co traced (tracer concentration < 35 kBq L^{-1} corresponding to a cobalt concentration of less than 2 x 10^{-12} mol L^{-1}) test solutions. Tracer ^{57}Co was used instead of ^{60}Co because the half life is shorter and the gamma decay energies are lower for ^{57}Co. The exemption value for ^{57}Co (102 Bq g^{-1}) is considerably higher than that of ^{60}Co (10 Bq g^{-1}) (STUK, ST1-5). Thus, for waste treatment reasons, using ^{57}Co is more preferred over the usage of ^{60}Co.

Batch sorption experiments were performed in 0.01 mol L^{-1} $NaNO_3$ solutions simulating simple aqueous nuclear wastes except from **article I** where the experiments were performed in aqueous solution containing only cobalt and EDTA. At least two parallel samples were prepared for every data point. The concentrations of stable cobalt varied between 2 µmol L^{-1} and 10 mmol L^{-1} and the concentration of EDTA varied between 0 µmol L^{-1} and 2 mmol L^{-1}. The test solutions were equilibrated in the dark over night with occasional mixing before measuring the test solution pH with an Orion 3 star

pH meter. The experiments were done at room temperature using constant rotary mixing (50 rpm) to equilibrate 20 mg of the sorbent material with 10 mL of the test solution (batch factor 500 mL g^{-1}) for 24 hours in the dark.

After mixing the suspensions, centrifugation (10 minutes at 4,000 rpm; 3,000×*g*) was used to remove the solid material from the solution. In addition, the solution was filtered with a 0.2 µm Acrodisc filter (PALL Life Sciences) in order to remove some very fine sorbent particles seen on the solution surface after centrifugation. To analyze the activity concentration of ^{57}Co in the solution, aliquots (5 mL) of the solution before and after the experiments were counted for ^{57}Co with a gamma counter (Wallac 1480 WizardTM 3 having a lead shielding). The solution aliquots were placed in 20 mL plastic bottles, the surface of which was wiped clean with ethanol before placing the bottles on the sample racks of the gamma counter. Each sample was counted for 30 minutes, or until a total amount of 100,000 counts had been accumulated. Considering the background count rate of approximately 20 cpm, a minimum detectable activity (MDA) of 0.08 Bq could be calculated for a typical measurement. This MDA is significantly lower than the remaining ^{57}Co activity in solution in any of the analyzed samples, allowing for the calculation of sorption distribution coefficients for all cobalt-containing samples. Thus, the distribution coefficient was used to estimate the processing capacity (L kg^{-1} or more commonly mL g^{-1}) of the sorbent material under the prevailing conditions. The accuracy of the results was evaluated using the propagation of uncertainty.

In order to analyze the possible effect of the used vials and syringe filters on the radioactivity concentration of the tracer, reference samples were used. The reference samples contained only the test solution and went through the same process as the actual samples. The tracer did not adhere on the surfaces of the used vials or filters.

3.3.2 UV EXPERIMENTS

Test solutions were prepared and analyzes of the samples were conducted following the same procedure as was described above for the batch experiments. The effect of UV irradiation on the sorption efficiency of the

synthesized titanium antimonates (unpublished results), antimony oxides in **article III and IV** and the commercial titania CoTreat® in **article I** was tested in a 100 mL immersion well reactor (Photochemical Reactors Ltd., Model 3312). A quartz tube separated the 6 W low-pressure mercury lamp (major emission wavelength of 254 nm) from the reaction mixture. The same batch factor (500 mL g^{-1}) was used in both, batch experiments and UV experiments. However, the amount of solid was 160 mg and the volume of test solution was 80 mL in the UV experiments. Parallel UV experiments were conducted only occasionally due to the length of each UV experiment.

A bubbling system delivering compressed air through sintered glass was used to stir the reaction mixture which was allowed to mix in the dark for one hour before the UV irradiation. Stirring was continued constantly during the experiments. The quartz immersion well used in the experiments was double-jacketed. The inner immersion well has a water inlet and outlet and a TTM-000 Series thermostat (TOHO Electronics Inc., Japan) was used for the circulation of cooling water and, thus, controlling the temperature (22-24 °C) during the experiments. Aliquots of 7 mL were taken from the reaction mixture at certain times and were centrifuged and filtered before pH and ^{57}Co activity measurements following the same procedure as was described above for batch experiment samples.

3.3.3 OZONATION EXPERIMENTS

Ozonation experiments were performed in a 250 mL reaction vessel using the residual ozone from a Wedeco Otsomatic Modular 4 HC-ozonator with 150 mL of solution with or without 300 mg of commercial titania, CoTreat®, and commercial titania photocatalyst, Degussa P25 TiO_2. The ozonator produced 4 g h^{-1} of ozone. The residual ozone originated from a gas mixture of ozone, oxygen and carbon dioxide while ozone was produced. The amount of the residual ozone in the gas mixture was not measured. Parallel ozonation experiments were done only occasionally due to the restricted possibility to conduct ozonation experiments.

4 RESULTS AND DISCUSSION

4.1 MATERIALS CHARACTERISATIONS

The commercial titania material, CoTreat®, is supplied in a mixed Na^+/H^+-form. According to published information, the Na^+-form contains 81.8% titania, 17.3% sodium oxide and silica as a minor component (about 1%) (Harjula et al., 2010). The analysis had been done as an external service by VTT, Finland using X-ray fluorescence (XRF) spectroscopy. Before the analysis, the titania material was first eluted with 0.1 mol L^{-1} nitric acid until the pH of the column effluent reached that of the influent (pH = 1.0). The Na^+-form was obtained by eluting the H^+-form first with 0.1 mol L^{-1} sodium hydroxide and then with 0.1 mol L^{-1} sodium nitrate until the pH of the column effluent was that of 0.1 mol L^{-1} sodium nitrate (pH 6.73). It was calculated that the sodium content of the Na^+-form was 5.60 mmol g^{-1}. The H^+-form contained 0.1 - 0.05 mmol g^{-1} sodium, thus more than 98% of sodium in CoTreat® was exchangeable to hydronium ions. The published XRD diffractogram of CoTreat® indicated that the material is poorly crystalline or nanocrystalline (Harjula et al., 2010). In this dissertation CoTreat® was tested in its as-supplied mixed Na^+/H^+-form in order to see the possible change of test solution pH caused by the material. The characteristics of CoTreat® was not analyzed further.

Based on the powder XRD patterns, the crystal phases of the synthesized materials were identified. TiSbA in **article II** was found to be a mixture of the pyrochlore (cubic, space group Fd_3m) and rutile titania (tetragonal, space group $P4_2/mnm$) structures. Based on the TiSbB powder XRD pattern in **article II**, the material has a mopungite type structure (tetragonal, space group $P4_2/m$). The crystal phase of both of the synthesized antimony oxides (**article III and IV**) resembled the pyrochlore type structure. In this thesis, the synthesized antimony oxides are referred to as antimony oxide-III and antimony oxide-IV (the material studied in **article III** and in **article IV**, respectively). The effect of UV irradiation on the bulk structure of the synthesized antimony oxides was also analyzed. A comparison of the

diffractograms of the materials before and after UV-C irradiation in $NaNO_3$ solution (0.01 mol L^{-1}) containing cobal (10 µmol L^{-1}) and EDTA (20 µmol L^{-1} in **article III** and 100 µmol L^{-1} in **article IV**) was conducted. The diffractograms before and after UV-C irradiation were identical, implying that UV irradiation has no effect on the bulk structure of the synthetic antimony oxides.

Analysis of the surface morphologies of the synthesized materials revealed that TiSbA and TiSbB resembled each other with the shape of the cubic like particles (Figure 11 and Figure 12, unpublished figures, FESEM images taken by L. Malinen). The surface roughness was more visible on TiSbB particles than on the TiSbA particles.

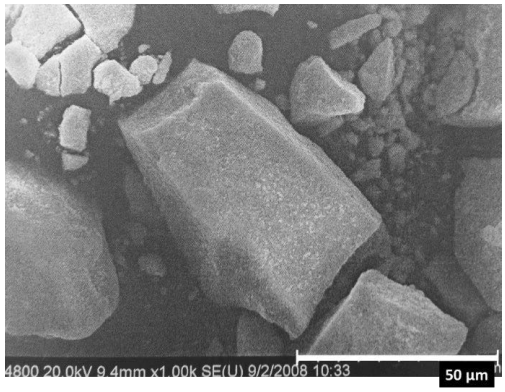

Figure 11 FESEM image illustrating the surface morpholoy of TiSbA (unpublished figure, image taken by L. Malinen).

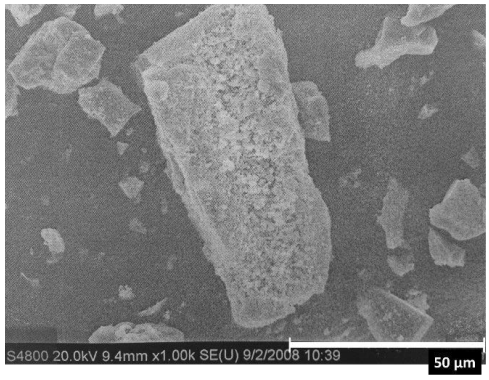

Figure 12 FESEM image illustrating the surface morphology of TiSbB (unpublished figure, image taken by L. Malinen).

In order to identify the elements present in TiSbA and TiSbB, an energy-dispersive X-ray spectroscopy (EDX) spectra was measured. Titanium was present in both of the materials even though its structural phase could not be seen in the XRD pattern of TiSbB. Since EDX measurements were performed from a powder-like sample, the values obtained should be considered estimates.

Analysis of the surface morphologies of the synthesized antimony oxides revealed the irregularity of the particles (FESEM images, Figure 13 and 14) in **article III and IV**.

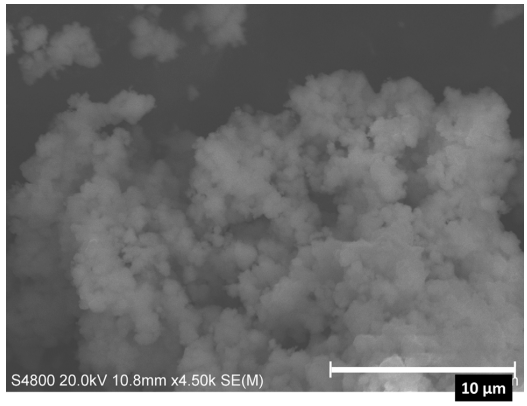

Figure 13 FESEM image illustrating the surface morphology of the synthesized antimony oxide-III.

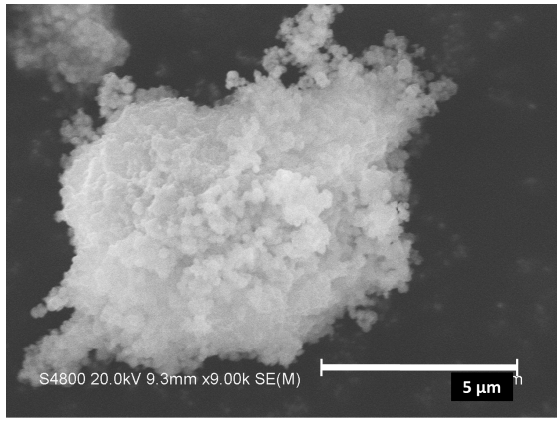

Figure 14 FESEM image illustrating the surface morphology of the synthesized antimony oxide-IV.

The specific surface areas and pore sizes of the synthesized materials can be found in Table 2.

Table 2 Specific surface area and total pore volume of the synthesized materials TiSbA and TiSbB (**article II**), antimony oxide-III (**article III**), and antimony oxide-IV (**article IV**).

Sorbent	Specific surface area ($m^2\ g^{-1}$)	Total pore volume ($cm^3\ g^{-1}$)
TiSbA	74 ± 4	0.200 ± 0.009
TiSbB	1 ± 0.1	0.011 ± 0,001
Antimony oxide-III	37 ± 2	0.140 ± 0.006
Antimony oxide-IV	49 ± 3	0.059 ± 0,003

Surface roughness has been shown to affect the accurate determination of the zeta potential when using the micro electrophoresis method (Delgado et al., 2005). Thus, the obtained zeta potential values (Figure 15) should be used only for the estimation of the point of zero charge (PZC) of the materials. The zeta potential values of the synthesized materials behave with a similar manner and the estimation of the PZC of the synthesized materials is below pH 2.5. Only cationic species should be retained on the charged surfaces of the materials above the PZC where the surface is negatively charged.

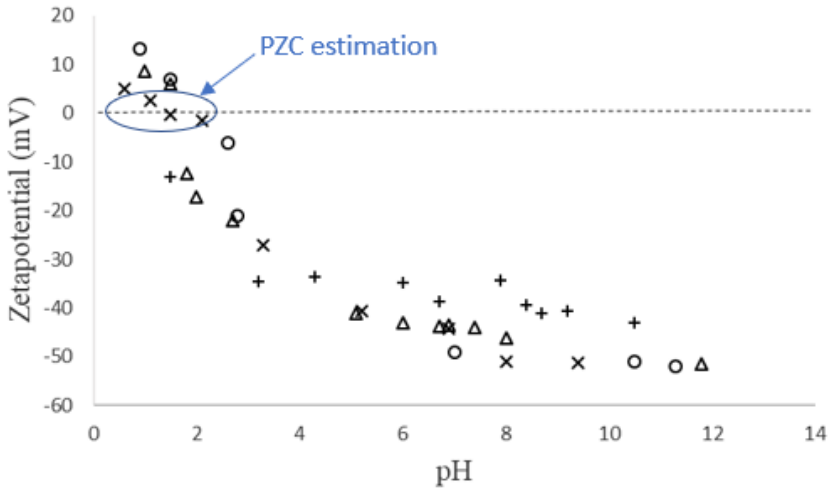

Figure 15 The zeta potential (mV) of TiSbA (○) and TiSbB (Δ) (**article II**), antimony oxide-III (+) (**article III**) and antimony oxide-IV (×) (**article IV**) as a function of the test solution pH after 24 hours of constant rotary mixing at room temperature in the dark with the synthesized material. The estimated PZC (point of zero charge) area has been marked with blue oval.

4.2 SEPARATION STUDIES

4.2.1 COMMERCIAL TITANIA, COTREAT®

The batch experiments were combined with different Advanced Oxidation Techniques when the removal of cobalt using the commercial titania, CoTreat®, was studied in **article I**. All the experiments presented in the article were conducted using EDTA (10 µmol L^{-1} unless mentioned otherwise) bearing solutions. At first, a batch sorption experiment without oxidation was conducted. Only a minor cobalt sorption capacity (7 ± 2% removal of cobalt) was obtained using CoTreat® with or without the commercial titania photocatalyst material Degussa P25 (Table 3). The solution used contained equimolar amount of cobalt and EDTA (10 µmol L^{-1} each) and the initial pH was 4.5.

Approximately 90 ± 1% of cobalt was removed when the suspension of CoTreat®, Degussa P25 and the cobalt-EDTA was UV irradiated for more than two hours (Table 3). The removal of cobalt was efficient (approximately 88 ± 1% removal) also when the EDTA concentration in the solution was increased

(50 μmol L^{-1}) indicating the efficiency of photocatalysis in the degradation of EDTA into species not able to bind cobalt in the solution.

When the effect of hydrogen peroxide was studied, a great surplus of hydrogen peroxide (1 mmol L^{-1}) over EDTA (10 μmol L^{-1}) was used. The suspension of CoTreat®, Degussa P25 and cobalt-EDTA was UV irradiated for two hours in the presence of hydrogen peroxide. After UV irradiation, about 85 ± 1% of cobalt was removed from the solution. Since the cobalt sorpion efficicency was lower than without the addition of hydrogen peroxide, it was concluded, that minor decomposition of CoTreat® was possible due to the addition of hydrogen peroxide in the solution.

When the suspension of CoTreat®, Degussa P25 and cobalt-EDTA was ozonated for four hours, 88 ± 1% removal of cobalt was achieved. A much higher sorption efficiency of cobalt was achieved when the process was divided in two stages. First, the cobalt-EDTA solution was ozonated without CoTreat® and Degussa P25. Secondly, after the ozonation, the solution was mixed with CoTreat® resulting in 96 ± 1% removal of cobalt.

Table 3 The removal of cobalt (%) and the equilibrium pH values for a solution containing cobalt (10 μmol L^{-1}) and EDTA (10 μmol L^{-1}) using different methods with and without the oxidation od EDTA and in the presence of the commercial titania CoTreat®, commercial titania photocatalyst Degussa P25, or their mixture.

The method used	Materials(s)	Removal of cobalt (%)	Equilibrium pH
24 h mixing without oxidation	CoTreat®	7 ± 2	7.1 ± 0.1
24 h mixing without oxidation	CoTreat® + Degussa P25	7 ± 2	7.0 ± 0.1
2 h UV	CoTreat®	16 ± 2	7.4 ± 0.1
2 h UV	Degussa P25	6 ± 2	7.4 ± 0.1
2 h UV	CoTreat® + Degussa P25	90 ± 1	7.0 ± 0.1
4 h ozonation	CoTreat® + Degussa P25	88 ± 1	7.0 ± 0.1
9 h ozonation + 24 h mixing	CoTreat®	96 ± 1	5.8 ± 0.1
9 h ozonation + 2 h UV	CoTreat® + Degussa P25	94 ± 1	5.0 ± 0.1
2 h UV + hydrogen peroxide	CoTreat® + Degussa P25	85 ± 1	6.5 ± 0.1

It has been reported that the decomposition of EDTA by ozonation is fast. When a solution containing EDTA (670 mg L^{-1}), cobalt sulphate (concentration not reported) and ^{60}Co as tracer (~1,000 Bq L^{-1}) was ozonated, two intervals of ozone uptake were distinguished (Seliverstov et al., 2009). The fast process (~20 min) corresponded to the oxidative decomposition of the major fraction of EDTA, while the slow process (subsequent ~40 min) corresponded to the reaction of ozone with the decomposition products of EDTA. The following reaction has been proposed for the ozonation of EDTA (Seliverstov et al., 2009):

(38) $$(CH_2COO^-)_2N - CH_2CH_2 - N(CH_2COO^-)_2 + 9O_3 \rightarrow$$
$$(intermediate\ oxidation\ products) \rightarrow 2NO_3^- + 2OH^- + 10CO_2 + 5H_2O + O_2$$

Based on the results achieved in **article I**, the effectiveness of the ozonation of EDTA was evident, even though residual ozone was used in the process. In **article I**, no additional benefit was obtained when the ozonated solution was UV irradiated together with CoTreat® and Degussa P25 (removal of cobalt 94%) instead of direct mixing with CoTreat® after the ozonation.

The cobalt sorption efficiency of another commercial titania, TiO_2 produced by Baker (99.9% w purity) has been tested in ^{60}Co solutions (63 MBq mg^{-1} cobalt nitrate with cobalt nitrate concentration of 1×10^{-2} mol L^{-1}) (Granados et al., 2006). The pH of the ^{60}Co solutions was 1, 3, 5, 7 or 10. The PZC of the titania was 6.7, thus, it was reported that the material should sorb only cationic species above pH 6.7. A sorption capacity of approximately 59% was achieved in the pH range between 6 and 7 (Granados et al., 2006). As a comparison, over 99% cobalt removal can be achieved using the titania, CoTreat®, in similar pH area when cobalt concentration was 10 μmol L^{-1} (Harjula et al., 1999 *a*). The removal of cobalt occurs through surface ion exchange mechanism when using the commercial titania produced by Baker (Granados et al., 2006). More specifically, the surface hydroxyl groups of the titania dissociate in TiO^-, which undergoes cation exchange. In the case of CoTreat®, it has been reported that the prevailing mechanism for trace transition metal uptake is surface complexation, rather than ion exchange

(Harjula et al., 2010). This was concluded from results where slope of 1 was obtained when the logarithmic value of the distribution coefficient was plotted as a function of solution pH. The slope of 1 indicates the exchange of univalent hydrolyzed species, e.g. $Co(OH)^{+}$ (Harjula et al., 2010). Based on calculations, cobalt was present in the solution below pH 6.5 as unhydrolyzed divalent cation, Co^{2+} (Harjula et al., 2010). Thus, the results indicated other sorption mechanism than ion exchange.

4.2.2 TITANIUM ANTIMONATES

When the removal of ionic cobalt was tested in batch experiment for the synthesized TiSbA and TiSbB titanium antimonates in **article II**, the sorption maximum for TiSbA was located at pH 4 and for TiSbB at pH 7. The difference of the pH values was explained by the difference of the synthesis conditions which were more alkaline in the case of TiSbB (pH 11.5) than in the case of TiSbA (pH about 2). The corresponding K_D values were 47,000 ± 500 mL g^{-1} (98.9 % removal of cobalt) and 38,000 ± 700 mL g^{-1} (98.7 % removal of cobalt), respectively. The results are in good correlation with published data of titanium antimonates synthesized using antimony pentachloride and titanium tetrachloride. About 90% removal of cobalt has been achieved in nitric acid solution (0.07 mol L^{-1}) in a test were titanium antimonite (0.10 g; Ti:Sb molar ratio 1.6 in synthesis) was equilibrated with 10 mL of nitric acid solution containing 0.1 mmol L^{-1} cobalt (metal ion from standard solution) (Chitrakar and Abe, 1986). When the logarithmic distribution coefficient, log K_D, values of the studied metal ions (e.g. Pb^{2+}, Fe^{2+} and Zn^{2+} in addition to Co^{2+}) were plotted against logarithmic nitric acid concentration, log[HNO_3], values a linear relationship with a slope of -2 was obtained (Chitrakar and Abe. 1986). This indicated that the sorption proceeded via ion exchange mechanism. Another researcher reported on results for a titanium antimonite material synthesized using the initial Ti:Sb molar ratio of 1.5 (Tsuji et al., 1993). Over 95% removal of cobalt was achieved in a batch experiment in nitric acid (concetration not specified) solution containing cobalt (0.1 equiv. dm^{-3} on titanium antimonate) (Tsuji et al., 1993). However, it should be noted that the batch factor in the two above mentioned researches was 100 mL g^{-1}.

When the effect of EDTA on the cobalt sorption efficiency of the titanium antimonite materials was reported in **article II**, it was noticed that at low pH values (below pH 2 after the experiment), an equimolar concentration of EDTA (10 μmol L^{-1}) did not have an effect on the removal of cobalt. However, it should be noticed that at pH 2, the amount of free cobalt ions in the solution is 66.9% (Gustafsson, Visual Minteq 3.0). In EDTA bearing solution, the cobalt sorption maximum for TiSbA was obtained at pH 2.6 and for TiSbB at pH 2.0. The corresponding K_D values were 5,400 ± 400 mL g^{-1} (91% removal of cobalt) and 17,900 ± 1,200 mL g^{-1} (97% removal of cobalt), respectively. The results indicated that the titanium antimonates either took up some of the various cobalt-EDTA species or removed Co^{2+} ions from the EDTA complexes (decomplexation). The possibility of the sorption of the EDTA complexes is discussed in more detail in chapter 4.2.3 Antimony oxides. In **article II**, the possibility of decomplexation was estimated using a rough calculation of cobalt distribution between the EDTA complexes and the titanium antimonate:

$$\frac{[CoEDTA^{2-}]}{C_S} = \frac{K_f}{K_D}[EDTA^{4-}] \quad (39)$$

where $[CoEDTA^{2-}]$ is the concentration of the $CoEDTA^{2-}$ complex, C_s is the concentration of sorbed Co^{2+} on the titanium antimonate, K_f is the formation constant of $CoEDTA^{2-}$, K_D is the distribution coefficient of Co^{2+} sorption on the titanium antimonate and $[EDTA^{4-}]$ is the concentration of $EDTA^{4-}$. According to the results practically all cobalt was sorbed as Co^{2+} by TiSbA at pH 2.6 and all cobalt was sorbed as Co^{2+} by TiSbB at pH 2.0.

Sodium nitrate (0,1 - 100 mmol L^{-1}) had varying effects on the synthesized titanium antimonates. When the concentration of sodium nitrate increased, the cobalt distribution coefficient values of TiSbA decreased and TiSbB slightly increased. This was explained by the competition between Co^{2+} and Na^{+} ions in the case of TiSbA at the equilibrium pH about 3. At such low pH area, there should still be some ionic cobalt present in the solution. The equilibrium pH for TiSbB was about 8. It was concluded that the increasing sodium

concentration was likely to decrease the negative surface charge of the material (see Figure 15) and thus facilitate the sorption of the negatively charged cobalt EDTA species, $CoEDTA^{2-}$.

Oxalic acid (1 - 100 mmol L^{-1}) had only a minor effect on the cobalt sorption efficiency of TiSbA when it was added in the EDTA bearing sodium nitrate solution. The excellent tolerance for oxalic acid of TiSbA was explained by the acidic (pH 2) synthesis conditions of the material. The equilibrium pH after batch experiment was at the same level as in the tests in sodium nitrate solutions regardless of the presence of oxalic acid. Since the equilibrium constants of cobalt-EDTA complexes are higher than those of cobalt-oxalic acid complexes, the effect of oxalic acid on the test conditions of TiSbA were minor. The situation was different with TiSbB. The presence of oxalic acid decreased the cobalt distribution coefficient values of the material considerably. In the EDTA bearing sodium nitrate solution the K_D value obtained at pH 2.7 was 3,600 ± 500 mL g^{-1}, whereas when oxalic acid was added, the highest K_D value obtained was 170 ± 10 mL g^{-1}. It was concluded that the surface of the TiSbB material was affected by oxalic acid.

4.2.3 ANTIMONY OXIDES

4.2.3.1 Batch experiments

In all the batch experiments presented in this section, the initial test solution pH was 4.5 – 5.5 and decreased to 3.1 – 2.8 during the experiments as a result of cobalt uptake by the ion exchanger and the subsequent release of protons in solution. This is an indication of the acidity of the synthesized antimony oxides. The acidity of hydrous oxides is known to increase with the order MO < M_2O_3 < MO_2 < M_2O_3 < MO_3 and the higher oxides of Sb^{5+} (present in Sb_2O_5 • 4 H_2O) exhibit good cation exchange properties at acidic pH (Abe, 1982). The cobalt sorption efficiency of both antimony oxides was strongly influenced by EDTA (Table 4).

Table 4 Distribution coefficient, K_D (mL g^{-1}), values obtained in batch experiments for the synthesized antimony oxides.

Solution component(s)	Material	K_D (mL g^{-1})
10 µmol L^{-1} cobalt	antimony oxide-III	140,000 ± 8,400
10 µmol L^{-1} cobalt and EDTA	antimony oxide-III	3,000 ± 100
10 µmol L^{-1} cobalt	antimony oxide-IV	19,300 ± 1,500
10 µmol L^{-1} cobalt and EDTA	antimony oxide-IV	1,700 ± 100

The experimental cobalt uptake values of antimony oxide-III and antimony oxide-IV in $NaNO_3$ solution with cobalt concentration varying between 2 µmol L^{-1} and 10 mmol L^{-1} are presented in Figure 16. The values were calculated based on the distribution coefficients values. The cobalt uptake values of antimony oxide-III rise with cobalt concentration and an S-shaped isotherm is formed, whereas the cobalt uptake reaches a plateau when antimony oxide-IV (Figure 16) is used. S-shaped isotherms may indicate a reversal in the selectivity of the material when polyfunctional ion exchangers (e.g. cation exchanger with sulfonic acid and carboxylic acid groups) are studied (Helfferich, 1962). Another possible explanation for an S-shaped isotherm is the following. When a small ion is exchanged by a larger one, the accommodation of the larger ion becomes more and more difficult as the exchange process proceeds. If steric hindrances are not formed and the exchange sites prefer the larger ion, it is possible that the larger ions are exchanged in places which are energetically less and less favorable or the lattice of the sorbent can be slightly distorted (Helfferich, 1962). When isotherm models are taken into account, it should be mentioned the the S-shaped isotherm of antimony oxide-III resembles the BET isotherm. The BET isotherm can be used for the determination of e.g. multilayer adsorption behavior, monolayer adsorption capacity and heat of adsorption at various adsorption layers (Ebadi et al., 2009). In **article III**, experimental sorption data was not analysed further and sorption isotherms were not fitted to the data.

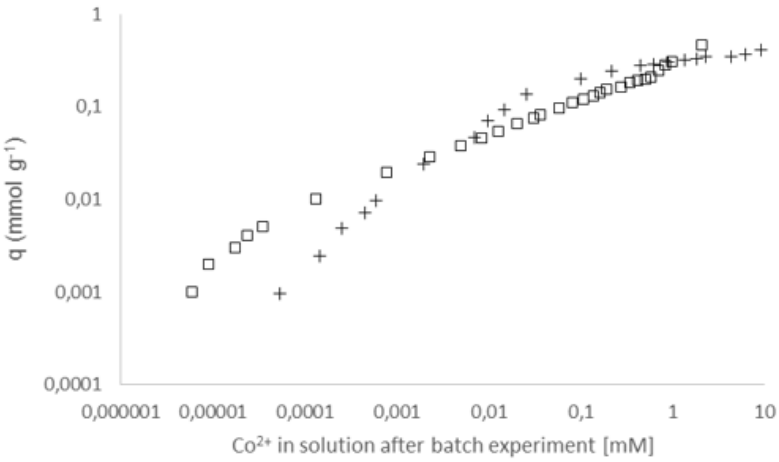

Figure 16 The uptake of Co^{2+}, q_e (mmol g^{-1}), in $NaNO_3$ solution containing varying concentration of Co^{2+} for antimony oxide-III (□) and antimony oxide-IV (+) as a function of the Co^{2+} concentration (mmol L^{-1}) in the solution after a batch experiment.

The experimental sorption data (Figure 16) was examined further for antimony oxide-IV by fitting six different isotherm models to the data. The equations and parameters of the models are presented in more detail in **article IV**. Here, only a brief explanation of the different models is given:

1) The Langmuir isotherm assumes that sorption takes place at specific homogenous sites of the sorbent without any mutual interactions between the sorbates.
2) The Freundlich isotherm is applicable for heterogeneous surfaces.
3) The Sips isotherm is a combination of the Langmuir and Freundlich isotherms and takes into account the surface heterogeneity.
4) The Toth model is an empirical equation, derived to improve the Langmuir model applicability at both low and high concentration limits and it is suitable in modeling of heterogeneous sorption processes.
5) The Dubinin-Radushkevich isotherm assumes a Gaussian energy distribution and includes the effect of temperature and it can be used to evaluate the sorption energies.

6) The BiLangmuir isotherm containing four parameters presumes that the sorbent surface has two Langmuir-like active sites with different affinities towards the target sorbing species.

The Sips model estimated the experimental sorption maximum with the highest accuracy and therefore was assigned to be the most suitable among the tested models. The good fit of the Sips model indicated that the synthesized antimony oxide-IV is a heterogeneous sorbent material, with different types of sorption sites. In the model the so called n_S value describes the surface heterogeneity (Kinniburg, 1986). When the n_S value deviates from unity, it denotes heterogeneous adsorbent surface. On the other hand, when the n_S value equals unity, the Sips isotherm returns to the Langmuir isotherm and indicates homogeneous adsorption (Kinniburgh, 1986). Thus, the heterogeneity of the synthesized antimony oxide-IV was also verified by the n_S value of 0.592 which is clearly less than unity.

The theoretical exchange capacity (Abe, 1987 and Baetsle and Huys, 1968) of $Sb_2O_5 \bullet 4\ H_2O$ is 5.06 meq g^{-1} which in the case of Co^{2+} corresponds to 2.5 mmol g^{-1}. However, according to experimental data (Abe and Sudoh, 1980), the maximum uptake of Co^{2+} by crystalline antimony oxide in 0.1 mol L^{-1} cobalt nitrate solution was found to be 0.61 meq g^{-1} corresponding 0.3 mmol g^{-1}. The value was obtained by equilibrating 20 mg of solid material and 20 mL of solution for 10 days. As can be seen in Figure 16, the Co^{2+} uptake of the synthesized antimony oxide-IV was in the same order of magnitude, 0.41 ± 0.07 mmol g^{-1}, in $NaNO_3$ solution containing 10 mmol L^{-1} cobalt. The Co^{2+} uptake of the antimony oxide-III was 1.5 ± 0.1 mmol g^{-1}. The rather low exchange capacity in comparison to the theoretical one, may arise from the strong hydration of small cations such as Co^{2+}, Ni^{2+} and Zn^{2+} (effective ionic radii being 0.745, 0.69 and 0.74 Å, respectively for coordination number VI) in aqueous solution (Shannon and Prewitt, 1969). It is possible that the hydration volumes of the cations contribute more to the steric effect than the crystal ionic radii. Thus, the theoretical exchange capacity may not be reached.

The ^{57}Co sorption efficiency of the synthesized antimony oxides was noticeably affected when cobalt was complexed with EDTA. The experimental

cobalt uptake values of antimony oxide-III and antimony oxide-IV in solution with cobalt concentration varying between 2 μmol L^{-1} and 1 mmol L^{-1} and EDTA concentration being two times higher than that of cobalt, are presented in Figure 17.

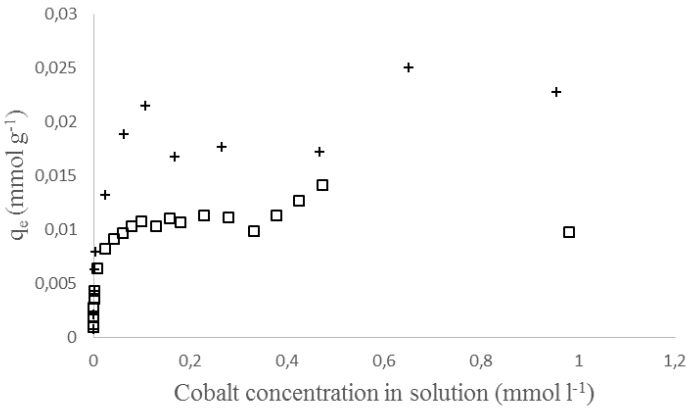

Figure 17 The uptake of Co^{2+}, q_e (mmol g^{-1}) in solution containing varying concentration of Co-EDTA complexes with the concentration of EDTA being two times higher than that of cobalt for antimony oxide-III (□) and antimony oxide-IV (+) as a function of the Co^{2+} concentration (mmol L^{-1}) in the solution after batch experiment.

The speciation of cobalt was estimated for the equilibrium pH values which were obtained in the test series presented in Figure 17 for antimony oxide-IV. The equilibrium pH of the solutions after batch experiment for the two antimony oxides differed from each other only 0.1 pH units. Thus the cobalt speciation presented in Table 5 is valid for the batch experiments of both materials.

Table 5 Calculated cobalt species for varying equimolar cobalt-EDTA solutions at the pH obtained after batch experiment (Gustafsson, Visual Minteq 3.0).

Solution			Speciation (%)			
Co^{2+} ($\mu mol\ L^{-1}$)	EDTA ($\mu mol\ L^{-1}$)	pH	Co^{2+}	$CoEDTA^{2-}$	$CoHEDTA^{-}$	CoH_2EDTA
2	**4**	**3.0**	5	31	60	4
5	**10**	**3.0**	2	32	62	4
10	**20**	**3.1**	1	37	58	3
15	**30**	**3.1**	0.5	38	58.5	3
20	**40**	**3.1**	0	38	59	3
50	**100**	**3.1**	0	38	59	3
100	**200**	**3.1**	0	38	59	3
150	**300**	**3.1**	0	38	59	3
200	**400**	**3.0**	0	32	63	5
300	**600**	**3.0**	0	32	63	5
500	**1000**	**3.0**	0	33	63	4
700	**1400**	**2.9**	0	27	67	6
1000	**2000**	**2.9**	0	28	66	6

The initial solution pH before the batch experiment was 4.5-5.5. It has been reported that at pH 5, EDTA appears in the solution mainly in the form of H_2EDTA^{2-} which reacts with Co^{2+} species in 1:1 molar ratio forming the negatively charged $Co(II)EDTA^{2-}$ complex (Smičiklas et al., 2006). According to the cobalt speciation at the equilibrium pH value (Table 5), it can be seen that cobalt is mainly complexed with EDTA throughout the test series. In **article II** and **III**, it was stated that the synthesized titanium antimonates or antimony oxide-III removed Co^{2+} from the metal EDTA complexes or that the materials were able to bind the species $CoEDTA^{2-}$ and $CoHEDTA^{-}$ which are present in the solution. When considering the possibility of the options, the stability constants of cobalt-EDTA complexes should be taken into account. The stability constants for $CoEDTA^{2-}$, $CoHEDTA^{-}$ and CoH_2EDTA are 18.16, 21.59 and 23.49, respectively (Martell, 1978 and Zachara et al., 2000), thus, the removal of Co^{2+} from the complexes could be considered less likely to occur

than binding the whole complexes on the surface of the antimony oxide. The adsorption of Me(II)EDTA^{2-} complexes on the surface hydroxyl (SOH) sites of sorbents at pH <5 can be explained by surface coordination following the equation (Zachara et al., 1995):

(40) $$SOH + H^+ + Co(II)EDTA^{2-}_{(aq)} = SOH_2^+ - Co(II)EDTA^{2-}$$

It is also possible, that the acidity of the antimony oxide materials creates acidic conditions on the solid-solution boundary affecting the cobalt speciation in solution. Thus, this solid/solution system should be considered as a multiple ligand system where EDTA and the surface of the antimony oxide compete for cationic cobalt.

The experimental sorption data scattered to some extent, especially for antimony oxide III but also for antimony oxide-IV, in the presence of EDTA as can be seen in Figure 17. Thus fitting the isotherm models to the data in **article IV** for antimony oxide-IV can be considered only as estimations. The Sips isotherm was the best estimation of the obtained experimental value, as was the case with the data obtained without the presence of EDTA.

In **article IV**, the energy values from the Dubinin-Raduschkevich model were used to evaluate the sorption mechanism. Energy values < 8 kJ mol^{-1} indicate physical sorption and values from 8 to 16 kJ mol^{-1} support ion exchange (Krishna et al., 2000 and Argun et al., 2007). For the solution containing only cobalt, the energy value was 6.2 kJ mol^{-1} and for the solution containing the cobalt-EDTA complexes, the energy value was 7.8 kJ mol^{-1}. The energy values indicate that the removal of Co^{2+} could be attributed to physical sorption. However, it has been reported that adsorption energy values as low as 0.6 kJ mol^{-1} have been obtained for ion exchange on zeolite clinoptilolite using the Dubinin-Radushkevich model (Inglezakis and Zorpas, 2012). In the research, a large number of experimental adsorption energy values were collected from the literature and 38% of the values were derived by the use of the Dubinin-Radushkevich model (Inglezakis and Zorpas, 2012). The maximum values obtained in **article IV** were very close to the proposed range of ion exchange (<16 kJ mol^{-1}) but the lower limit was not accurate. The

correlation coefficients for the Dubinin-Radushkevich model in **article IV** were 0.978 and 0.755. The accuracy of the obtained energy values in **article IV** and the above-mentioned low energy values representing ion exchange mechanism (0.6 kJ mol^{-1} by Inglezakis and Zorpas, 2012) should be taken into account when conclusions are made based on the results. Thus, critical evaluation is needed before suggesting that the reaction mechanism for cobalt removal in **article IV** could be physical sorption.

4.2.3.2 Sorption experiments with UV irradiation

The potentially photocatalytic nature of the synthesized antimony oxides and the possible photodegradation of EDTA were studied with the sorption experiments with UV irradiation. The main aim of the experiments was to analyze the influence of UV irradiation on cobalt uptake of the materials, thus, only radiochemical analyses on the amount of ^{57}Co were conducted. The usefulness of EDTA analyses is discussed in the Conclusions-chapter of the dissertation. The sorption investigations were conducted in the absence and presence of EDTA.

When the EDTA bearing solution was UV irradiated in the presence of antimony oxide-III, the obtained distribution coefficient was more than 5 times smaller than that obtained in the batch experiment without EDTA but increased noticeably compared to the experiment made in the dark in the EDTA bearing solution (Figure 18).

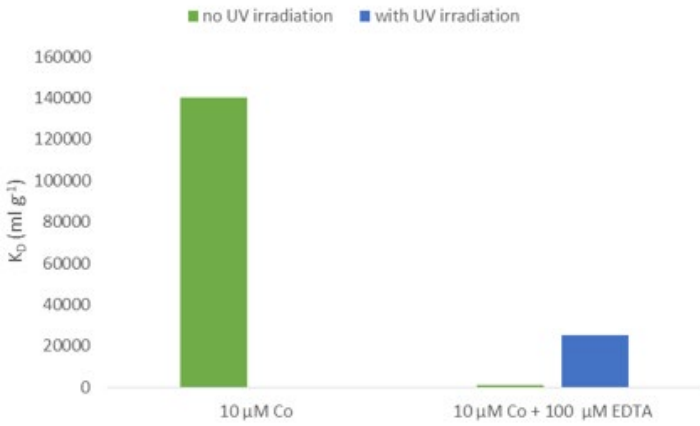

Figure 18 Sorption distribution coefficients (K_D) of the test solutions in the absence and presence of EDTA without (green column) and with (blue column) 6 hours of UV irradiation for antimony oxide-III.

In the case of antimony oxide-IV, the sorption distribution coefficient value (K_D, mL g^{-1}) in the solution containing only ionic cobalt was significantly increased due to UV irradiation compared to the one obtained without UV irradiation (Figure 19). Unfortunately, an UV experiment without EDTA was not conducted for antimony oxide-III, thus, this interesting phenomenon cannot be compared between the two antimony oxides. It was concluded in **article IV**, that the sorption increase in the presence of UV irradiation could be related to a change in cobalt speciation, most likely the oxidation of Co^{2+} to Co^{3+}. The oxidation could have occurred due to the photocatalytic activity of the synthesized antimony oxide-IV or the formation of solution radicals by the external light source.

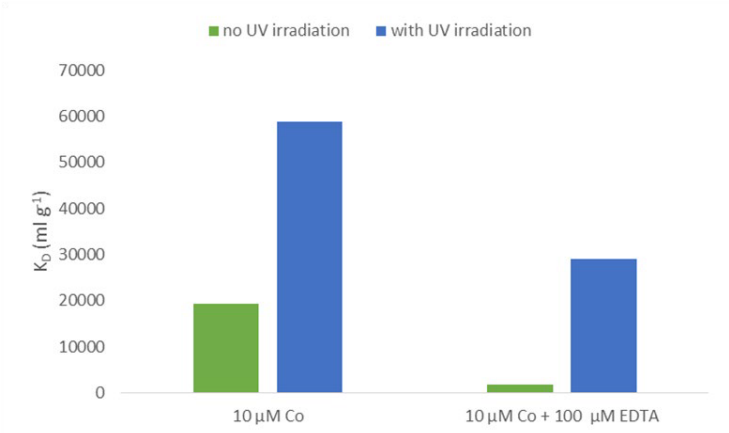

Figure 19 Sorption distribution coefficients (K_D) of the test solutions in the absence and presence of EDTA without (green column) and with (blue column) 24 hours of UV irradiation for antimony oxide-IV.

The possible oxidation of Co^{2+} to Co^{3+} under UV irradiation has been reported to occur above pH 7 (Rekab et al., 2015). An UV source with photonic power of 17 W (254 nm) was used to irradiate cobalt-EDTA solutions for 3 hours. When the precipitation of cobalt under UV irradiation was studied, it was noticed that precipitation took place at lower pH values (at pH 8-9) than without UV irradiation (pH 10-11) (Rekab et al., 2015). This was explained by the fact that Co^{3+} precipitates at a lower pH than Co^{2+}. The oxidation did not involve reduction of nitrates (identical results were obtained with cobalt chloride and nitrate) thus the oxidation was caused only by the UV irradiation.

The oxidation of Co^{2+} in water has been proposed to follow the reaction (Eaton and Stuart, 1968):

(41) $$Co^{2+} + H_2O \rightarrow Co^{3+} + OH^- + \frac{1}{2}H_2$$

In **article III** and **IV**, a 6 W UV source was used and the solution was lower than in the above-mentioned research about Co^{2+} oxidation under UV irradiation. Despite the differences, the possibility of Co^{2+} oxidation to Co^{3+} should be taken into account. The possibility that the solution could contain Co^{3+}, could affect the removal of cobalt. The stability constant, log K, for the Co^{3+}-EDTA complexes is over 40 (Martell and Smith, 1977), which is considerably higher than that of Co^{2+}-EDTA complexes (see Table 6).

Table 6 Aqueous complexation reactions of Co^{2+} with EDTA (Martell and Smith, 1977).

Reaction equation	log K
$EDTA^{4-} + Co^{2+} = CoEDTA^{2-}$	18.16
$EDTA^{4-} + Co^{2+} + H^{+} = CoHEDTA^{-}$	21.59
$EDTA^{4-} + Co^{2+} + 2H^{+} = CoH_2EDTA$	23.49

In **article III** and **IV**, the distribution coefficient value, K_D, of the antimony oxide suspension containing both cobalt and EDTA increased due to UV irradiation compared to the non-irradiated EDTA-containing solution (Figure 18 and 19). In **article IV** the K_D value for UV-irradiated EDTA-bearing solution is even higher than that obtained in the solution containing only ionic cobalt that has not been exposed to UV irradiation. This wasn't seen in **article III**. However, it should be mentioned that the results of the UV experiments are not directly comparable between **article III** and **IV**, since different UV irradiation times were used (6 hours and 24 hours, respectively). The results in **article IV** imply that degradation of EDTA has occurred in combination with cobalt oxidation. However, it is possible that the oxidation has not progressed to the same extent as observed in the EDTA-free solution under UV irradiation (where the highest K_D value was obtained). Another explanation is that some of the EDTA has not photodegraded and cobalt remained in the solution complexed with EDTA, at least to some extent.

The photocatalytic activity of hydrous antimony oxides synthesized from antimony trioxide, water and varying volumes of hydrogen peroxide (added dropwise) has been studied (Chen et al., 2017). In the study three 4 W UV lamps (254 nm) were used and the oxidation of gaseous benzene was studied. According to the results, highest oxidation rate of benzene was achieved with the material with the highest BET surface area (38.2 $m^2\ g^{-1}$). Reactive oxygen species were detected in the study, and it was concluded that the large amount of $O2^{\bullet-}$ and •OH on the surface of the hydrous antimony oxide under UV irradiation was the main reason for the good photocatalytic activity. The obtained mineralization rates of benzene were higher than those of the commercial titania photocatalyst, TiO_2 P25 (Chen et al., 2017). As a

comparison, in **article III** the BET surface area of the synthesized antimony oxide-III was 37 ± 2 m^2 g^{-1}, and in **article IV** the BET surface area of the synthesized antimony oxide-IV was 49 ± 3 m^2 g^{-1}. Thus, these values imply high photocatalytic activity for the oxidation of EDTA.

4.2.3.3 Effect of interfering ions without UV irradiation

In **article IV**, the selectivity between the divalent ions of cobalt, calcium and nickel was studied for the synthesized antimony oxide-IV. As has been mentioned earlier, calcium and nickel ions are generally present in the NPP liquid waste and can have an interfering effect on the cobalt removal efficiency of the sorbent materials. The studies were conducted in the presence (100 μmol L^{-1}) or absence of EDTA with and without UV irradiation. The solutions contained 10 - 1,000 μmol L^{-1} calcium or nickel. The uptake of cobalt decreased by a factor of more than three in the presence of 10 - 100 μmol L^{-1} calcium or nickel without EDTA. It was concluded that at these concentrations, the sorption is still within the ideal sorption range of the antimony oxide-IV. The selectivity of calcium and nickel over cobalt was explained by the sorption on the "strong" sorption sites which are active at the sorption range (below 100 μmol L^{-1}). The preference towards cobalt increased together with the increase of the competing metal ion concentration. When the competing metal ion concentration was 1,000 μmol L^{-1}, the cobalt uptake was almost as high as the uptake in the absence of any competing metal ions. When the concentration of metal ions increases in the solution, the sorption occurs in the non-ideal sorption range, where "weak" sorption sites are responsible for the uptake of metal ions from solution. The weak sites seemed to have no preference for calcium or nickel over cobalt in **article IV**. Both competing metals, calcium and nickel, affected the removal of cobalt in a very similar fashion. As for author's knowledge, the selectivity of antimony oxide between calcium and cobalt has not been published. Some literature on the selectivity between nickel and cobalt can be found. It has been reported that crystalline antimony oxide is more selective towards Co^{2+} than Ni^{2+} in nitric acid solutions containing 100 μM metal ions (Abe and Kasai, 1979).

When EDTA was added to the Ca^{2+} bearing solution, the cobalt sorption efficiency of antimony oxide-IV was even lower than in the presence of EDTA only. This was explained by the smaller calcium-EDTA stability constants in comparison to the cobalt-EDTA stability constants (see Table 7). At pH values below 3.5, calcium is in free ionic form (Gustafsson, Visual Minteq 3.0) and only cobalt forms complexes with EDTA. Thus, free calcium ions are adsorbed on the antimony oxide resulting in a lower cobalt distribution coefficient values in the presence of calcium. The cobalt distribution coefficient increased with increasing calcium concentration in a similar way which was seen in the solutions without EDTA. It was concluded in **article IV** that the overall cobalt uptake of cobalt at these high calcium concentrations was influenced only by EDTA and the formation of soluble cobalt-EDTA complexes in solution.

Table 7 Aqueous complexation reactions of Ca^{2+} and Ni^{2+} with EDTA (Martell and Smith, 1977).

Reaction equation	log K
$EDTA^{4-} + Ca^{2+} = CaEDTA^{2-}$	12.44
$EDTA^{4-} + Ca^{2+} + H^{+} = CaHEDTA^{-}$	15.97
$EDTA^{4-} + Ni^{2+} = NiEDTA^{2-}$	20.11
$EDTA^{4-} + Ni^{2+} + H^{+} = NiHEDTA^{-}$	23.64
$EDTA^{4-} + Ni^{2+} + 2H^{+} = NiH_2EDTA$	24.74

In the nickel and EDTA containing solutions, only the lowest concentration (10 µmol L^{-1}) of nickel decreased the cobalt uptake in a similar manner as was noted for calcium in **article IV**. When the concentration of nickel increased, the effect of nickel on the sorption efficiency of antimony oxide-IV almost completely disappeared. This could be explained by the relative stabilites of the divalent metal ion complexes with EDTA (see Table 6 and 7), which are higher for nickel EDTA complexes.

4.2.3.4 Effect of interfering ions under UV irradiation

The effect of interfering ions, calcium and nickel, under UV irradiation was studied in **article IV**. The results are presented in Figure 20. It should be noted, that also the earlier discussed results for solution containing only ionic

cobalt or both, cobalt and EDTA, are included in Figure 20 in order to be able to compare the results in an easier way.

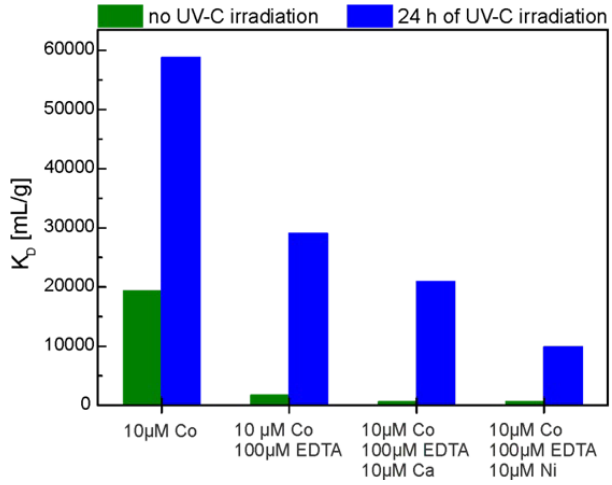

Figure 20 Sorption distribution coefficient values (K_D) of the test solutions in the absence and presence of EDTA without (green column) and with (blue column) 24 hours of UV irradiation (as presented in **article IV**).

The distribution coefficient, K_D, in the calcium bearing solution is higher than for ionic cobalt solution without UV irradiation but much lower than that of cobalt bearing solution under UV irradiation. This implies that the earlier discussed possible cobalt oxidation (from Co^{2+} to Co^{3+}) takes place at the surface of the antimony oxide and not in solution. Calcium cannot be oxidized to a higher oxidation state in aqueous solution. Thus, it was concluded in **article IV**, that the obtained distribution coefficient under UV irradiation can be explained by partial oxidation of cobalt and degradation of EDTA. However, the sorption sites on the surface of the antimony oxide are occupied by calcium lowering the possibility of oxidation of cobalt. This leads to the decrease on the cobalt uptake in calcium bearing solution.

The presence of nickel affected the sorption of cobalt more than the presence of calcium (see Figure 20). In **article IV**, it was stated that in the presence of nickel, additional reactions must occur which are absent in the presence of calcium. It is possible that the reactions are related to the redox behaviour of nickel and the production of other oxidation states than Ni^{2+}. For example, the Ni^{3+} ion could be capable of suppressing the sorption of Co^{2+} on

the surface of tha antimony oxide and the subsequent oxidation of Co^{2+} to Co^{3+}. It has been reported that Ni^{2+} oxidation can take place on the hematite surface after photoexcitation of hematite (α-Fe_2O_3) (Wang et al., 2013). It is expected that any free, non-complexed (i.e. surface sorbed or EDTA associated) Co^{3+}/Ni^{3+} would undergo immediate reduction to Co^{2+} and Ni^{2+} after the UV treatment when taking into account the stability fields of the various species in aqueous solution (Rekab et al., 2015, and Beverskog and Puigdomenech 1997). It was discussed in **article IV**, that eventhough UV irradiation enhanced the selectivity of antimony oxide-IV between cobalt and nickel, nickel clearly interferes with the removal of cobalt.

5 CONCLUSIONS AND OUTLOOK

In this thesis a rather wide variety of different types of sorption experiments were conducted for the commercial titania CoTreat®, synthesized titanium antimonates and synthesized antimony oxides. It was concluded that CoTreat® is not suitable for a single-stage process in the presence of EDTA. However, high cobalt sorption efficiency was achieved when EDTA was first oxidized by utilizing Advanced Oxidation Technologies.

Titanium antimonates were tested in acidic solutions and good cobalt distribution coefficient values we obtained. Interestingly it was noticed that the materials were quite likely able to adsorb also the cobalt-EDTA complex.

UV irradiation clearly increased the cobalt sorption efficiency of the synthesized antimony oxide-IV. The positive effect of UV irradiation was also clear in the EDTA bearing solution for the antimony oxide-III. The remarkable increase in the distribution coefficients of antimony oxide-IV under UV irradiation imply that the material could be photocatalytically active. Antimony oxides could also be considered suitable for a single-stage process when the solution pH is below 5. No additional oxidizer, like e.g. H_2O_2, was used in the experiments. This can be considered highly beneficial since the addition of each chemical in the treatment system complicates the system to some extent.

Additional analysis methods, like chromatographic or capillary electrophoresis determination, for the measurement of the degradation rate of EDTA would have been highly appreciated for the analysis of the results. However, at the time of the experiments, these analysis methods had to be left out of the study, since radioactive solutions were used and suitable analysis instruments were not available for such analysis. It was also decided, that due to the rather time consuming experiments (maximum three UV irradiation experiments in a week), solutions without radioactive tracer were not used. However, the analysis of the degradation rate should be done in the future.

When considering a typical NPP floor drain water effluent, the activation corrosion products (e.g. nickel and cobalt) are present in trace concentrations

and calcium accounts for the majority of the divalent metal ion concentration. When the calcium concentration is in the millimolar concentration range, the cobalt removal efficiency of the antimony oxide-IV should not be hampered which emphasizes its suitability for the purification of aqueous nuclear waste. However, it should be mentioned that the situation was somewhat different for waste solutions that contain EDTA, since the effect of calcium was evident in EDTA bearing solutions also in the millimolar concentration range.

UV irradiation can be considered as an efficient addition for the cobalt sorption process with antimony oxides. According to the XRD analysis, the bulk structure of the synthesized antimony oxides showed no changes during UV irradiation, which emphasized the usability of the material in liquid waste treatment systems utilizing UV irradiation.

It is possible to remove particulate cobalt from NPP effluents by filtration but the soluble forms of cobalt require the use of e.g. precipitation or ion exchange. A rather difficult waste form, radioactive sludge, is produced in the precipitation process. Sludge contains also inactive metals and usually requires solidification in e.g. cement, to be suitable for final disposal. Using selective sorbent materials results in a smaller amount of solid waste as the accumulation of inactive metals is avoided and only target radionuclide is removed from the effluent.

In addition to the analysis on EDTA concentration in the solutions, in the case of antimony oxide, also the concentration of calcium and nickel should be analyzed in further studies. This would enable understanding the sorption behaviour and possible oxidation of the solution components. The future studies should, thus, include also investigations of the redox chemistry of the involved elements. It would also be beneficial to include iron in the future studies as an additional interfering ion.

REFERENCES

Abe, M. (1987) Ion exchange selectivities of crystalline antimonic acid, in Recent Developments of Ion Exchange, Williams, P. A. and Hudson, M. J. (editors), Elsevier Applied Science, London and New York.

Abe, M. (1982) Oxides and hydrous oxides of multivalent metals as inorganic ion exchangers. In: Clearfield, A. (ed) Inorganic Ion Exchange Materials, CRC Press, Boca Raton, Florida.

Abe, M., Chitrakar,R., Tsuji, M., Fukumoto, K. (1985) Synthetic inorganic ion-exchange materials XXXIX. Synthesis of titanium(IV) antimonates and their ion exchange properties for alkali and alkaline earth metal ions. Solv. Extr. Ion Exch. 3(1&2):149-172.

Abe, M., Ito, T. (1968) Synthetic inorganic ion-exchange materials. X. Preparation and properties of so-called antimonic(V) acid. Bull. Chem. Soc. Japan 41:333-342.

Abe, M., Kasai, K. (1979) Synthetic inorganic ion-exchange materials. XXII. Distribution coefficients and possible separation of transition metals on crystalline antimonic(V) acid as a cation exchanger. Sep. Sci. Technol. 14:895-907.

Abe, M., Sudoh, K. (1980) Synthetic inorganic ion-exchange materials. XXIII. Ion-exchange equilibria of transition metals and hydrogen ions on crystalline antimonic(V) acid. J. Inorg. Nucl. Chem. 42:1051-1055.

Abe, M., Tsuji, M. (1983) Synthesis of quadrivalent metal antimonates as ion exchangers and their selectivities for alkali metal ions. Chem. Letters 1561-1564.

Andreozzi, R., Caprio, V., Insola, A., Marotta, R. (1999) Advanced oxidation processes (AOP) for water purification and recovery. Catalysis Today 53:51-59.

Andreozzi, R., Insola, A., Caprio, V., D'Amore, M. G. (1992) The kinetics of Mn(II)-catalysed ozonation of oxalic acid in aqueous solution. Wat. Res. 26(7):917-921.

Argun, M. E., Dursun, S., Ozdemir, C., Karatas, M. (2007) Heavy metal adsorption by modified oak sawdust: Thermodynamics and kinetics. J. Haz. Mat. 141:77-85.

Babay, P. A., Emilio, C. A., Ferreyra, R. E., Gautier, E. A., Gettar, R. T., Litter, M. I. (2001) Kinetics and mechanisms of EDTA photocatalytic degradation with TiO_2 under different experimental conditions. Int. J. Photoen. 3:193-199.

Baetsle, L. H., Huys, D. (1968) Structure and ion exchange characteristics of polyantimonic acid. J. Inorg. Nucl. Chem. 30:639-649.

Bains, N., Goosey, M., Hayer, R. (2003) Evaluation of an enhanced oxidation method for the destruction of ethylene diamine tetra-acetic acid (EDTA) and related compounds in aqueous solution. Circuit World 29:15-19.

Bergers, P. J. M., De Groot, A. C. (1994) The analysis of EDTA in water by HPLC. Wat. Res. 28(3):639-642.

Beverskog, B., Puigdomenech, I. (1997) Revised Pourbaix diagrams for nickel at 25-300^{0}C. Corrosion Sci. 39:969-980.

Blok, J., Frattini, P., Moser, T. (2002) Advances in ultrasonic fuel cleaning. In, IAEA INIS collection public web pages, Report FRO301239, accessed 6th June, 2019: https://inis.iaea.org/collection/NCLCollectionStore/_Public/34/066/34066631.pdf.

Bucheli-Witschel, M., Egli, T. (2001) Environmental fate and microbial degradation of aminopolycarboxylic acids. FEMS Microbiol. Rev. 25:69-106.

Chen, J., Chen, Z., Zhang, X., Li, X., Yu, L., Li, D. (2017) Antimony oxide hydrate ($Sb_2O_5 \cdot 3H_2O$) as a simple and high efficient photocatalyst for oxidation of benzene. Appl. Catal. B: Environ. 210:379-385.

Chitrakar, R., Abe, M. (1986) Synthetic inorganic ion-exchange materials. XLII. Ion-exchange selectivity of divalent transition metals and lead on titanium antimonate and some chromatographic separations. Analyst. 111:339-343.

Choppin, G., Liljenzin, J.-O., Rydberg, J., Ekberg, C. (editors) (2013) Radiochemistry and nuclear chemistry, Elsevier Inc., Amsterdam, Boston, Heidelberg, London, New York, Oxford, Paris, San Diego, San Francisco, Sydney and Tokyo.

Chu, S. Y. F., Ekström, L. P., Firestone, R. B. (1999) The Lund/LBNL nuclear data search. Version 2.0, www.nucleardata.nuclear.lu.se/toi/, accessed 8th August, 2019.

Clearfield, A. (2000) Inorganic ion exchanger, past, present and future. Solv. Extr. Ion Exchange 18(4): 655-678.

Delgado, A. V., González-Caballero, F., Hunter, R. J., Koopal, L. K., Lyklema, J. (2005) Measurement and interpretation of electrokinetic phenomena. Pure Appl. Chem. 77(10):1753-1805.

Diebold, U. (2003) The surface science of titanium dioxide. Surf. Sci. Rep. 48:53-229.

Eaton, D. R., Suart, S. R. (1968) Electron spin resonance studies of the photooxidation and reduction of cobalt complexes. J. Phys. Chem. 72(2)400-405.

Ebadi, A. E., Mohammadzadeh, J. S. S., Khudiev, A. (2009) What is the correct form of BET isotherm for modeling liquid phase adsorption? Adsorption 15:65-73.

Fujishima, A., Rao, T. N., Tryk, D. A. (2000) Titanium dioxide photocatalysis. J. Photochem. Photobiol. C: Photochem. Rev. 1:1-21.

Fujiwara, K., Kawamura, H., Kanbe, H., Hirano, H., Takiguchi, H., Yoshino, K., Yamamoto, S., Shibata, T., Ishigure, K. (2006) Applicability of chemical cleaning process to steam generator secondary side, (IV) Comprehensive applicability evaluation of chemical cleaning and its effect on integrity of other structural materials other than steam generator tubes. J. Nucl. Sci. Tech. 43(11):1344-1358.

Furia, T. E. (1972) Sequestrants in foods, in CRC Handbook of Food Additives, 2nd edition, Furia, T. E. (ed), CRC Press, Boca Raton, London, New York and Washington, D. C.

Gardoni, D., Vailati, A., Canziani, R. (2012) Decay of ozone in water: A review. Ozone: Sci. Eng. 34:233-242.

Gerischer, H., Heller, A. (1991) The role of oxygen in photooxidation of organic molecules on semiconductor particles. J. Phys. Chem. 95:5261-5267.

Glaze, W. H., Kang, J.-W., Chapin, D. H. (1987) The chemistry of water treatment processes involving ozone, hydrogen peroxide and ultraviolet radiation. Ozone Sci. Eng. 9:335-352.

Granados, F., Bertin, V., Bulbulian, S., Solache-Ríos, M. (2006) ^{60}Co aqueous speciation and pH effect on the adsorption behavior on inorganic materials. Appl. Rad. Isot. 64:291-297.

Grygar, T., Zmitko, M. (2002) Corrosion products behaviour under VVER primary coolant conditions In, OSTI public web pages, Report INIS-FR-1539, accessed 23rd February, 2020: https://www.osti.gov/etdeweb/servlets/purl/20377576

Gustafsson, J. P. Visual Minteq 3.0, a free equilibrium speciation model. Accessed 27th June, 2016: http://vminteq.lwr.kth.se/.

Hanaor, D. A. H., Sorrell, C. C. (2011) Review of the anatase to rutile phase transformation. J. Mater. Sci. 46:855-874.

Harjula, R., Kelokaski, M., Leinonen, H. (2010) Sorption of radiocobalt and other activated activation product radionuclides on titanium oxide material CoTreat. Radiochim Acta 98:341-345.

Harjula, R., Lehto, J., Paajanen, A., Brodkin, L., Tusa, E. (1999 *a*) Removal of radiocobalt and other activated corrosion product nuclides from NPP waste waters by highly selective CoTreat ion exchange media. In: Proceedings of the 7th

International Conference on Radioactive Waste Management and Environmental Remediation, ASME 1999, Nagoya, Japan.

Harjula, R., Lehto, J., Paajanen, A., Brodkin, L., Tusa, E. (1999 *b*) Testing of highly selective CoTreat ion exchange media for the removal of radiocobalt and other activated corrosion product nuclides from NPP waste waters. In: Proceedings of Waste Management, 1999, Tucson, AZ, United States.

Helfferich, F. (ed) (1995) Ion Exchange, Dover Publications, Inc., New York.

Hurum, D. C., Agrios, A. G., Gray, K. A., Rajh, T., Thurnauer, C. (2003) Explaining the enhanced photocatalytic activity of Degussa P25 mixed-phase TiO_2 using EPR. J. Phys.Chem. B 107:4545-4549.

Inglezakis, V. J., Poulopoulos, S. G. (eds) (2006) Adsorption, Ion Exchange and Catalysis, 1st Edition, Design of Operations and Environmental Applications, Elsevier, Oxford, UK.

Inglezakis, V. J., Zorpas, A. A. (2012) Heat of adsorption, adsorption energy and activation energy in adsorption and ion exchange systems. Desal. Water Treat. 39:149-157.

Karhu, P., Möller, T., Harjula, R., Lehto, J. (2000) Titanium antimony oxides: synthesis and ion exchange properties for radioactive caesium, strontium and cobalt, Ion exchange at the millennium. In: Proceedings of IEX 2000, Imperial College Press, London, 109-115.

Kari, F. G., Giger, W. (1995) Modeling the photochemical degradation of ethylenediaminetetaacetate in the River Glatt. Environ. Sci. Technol. 29:2814-2827.

Karunakaran, C., Narayanan, S., Gomathisankar, P. (2010) Photocatalytic degradation of 1-naphtol by oxide ceramics with added bacterial disinfection. J. Haz. Mat. 181:708-715.

Khan, A. A., Alam, M.M. (2004) New and novel organic-inorganic type crystalline ´polypyrrolel/polyantimonic acid' composite system: preparation, characterization and analytical applications as a cation-exchange material and Hg(II) ion-selective membrane electrode. An. Chim. Acta 504:253-264.

Kinniburgh, D. G. (1986) General purpose adsorption isotherms. Environ. Sci. Technol. 20:895-904.

Kinnunen, P. (2008) ANTIOXI Decontamination techniques for activity removal in nuclear environments, VTT Research Report, NO VTT-R-00299-08, Espoo, Finland.

Koivula, R., Pakarinen, J., Sivenius, M., Sirola, K., Harjula, R., Paatero, E. (2009) Use of hydrometallurgical wastewater as a precursor for the synthesis of cryptomelane-type manganese dioxide ion exchange material, Sep. Pur. Technol. 70:53-57.

Krapfenbauer, K., Getoff, N. (1999) Comparative studies of photo- and radiation-induced degradation of aqueous EDTA. Synergistic effects of oxygen, ozone and TiO_2 (acronym: CoPhoRaDe/EDTA). Radiat. Phys. Chem. 55:385-393.

Krishna, B. S., Murty, D. S. R., Prakash Jai, B. S. (2000) Thermodynamics of chromium(VI) anionic species sorption onto surfactant-modified montmorillonite clay. J. Colloid Interf. Sci. 229:230-236.

Kunz, A., Peralta-Zamora, P., Durán, N. (2002) Hydrogen peroxide assisted photochemical degradation of ethylenediaminetetraacetic acid. Adv. Environ. Res. 7:197-202.

Lin, C. C. (2009) A review of corrosion product transport and radiation field buildup in boiling water reactors. Prog. Nucl Energy 51:207-224.

Luttrell, T., Halpegamage, S., Tao, J., Kramer, A., Sutter, E., Batzill, M. (2014) Why is anatase a better photocatalyst than rutile? - Model studies on epitaxial TiO2 films. Nature Scientific Reports. 4:4043.

Madden, T., Datye, A.K., Prairie, M. R., Stange, B. M. (1996) Evaluation of the treatment of metal-EDTA complexes using TiO_2 photocatalysis. Solar Eng. 71:78.

Martell, A. E., Smith, R. M. (editors) (1977) Critical Stability Constants. Vol. 3. Plenum, New York.

Means, J. L., Crerar, D. A., Duguid, J. O. (1978) Migration of radioactive wastes: Radionuclide mobilization by complexing agents. Science. 200(4349):1477-1481.

Metsärinne, S., Tuhkanen, T., Aksela, R. (2001) Photodegradation of ethylenediaminetetraacetic acid (EDTA) and ethylenediamine disuccinic acid (EDDS) within natural UV radiation range. Chemosphere. 45:949-955.

Möller, T., Harjula, R., Kelokaski, P., Vaaramaa, K., Karhu, P., Lehto, J. (2003) Titanium antimonates in various Ti:Sb ratios: ion exchange properties for radionuclide ions. J. Mater. Chem. 13:535-541.

Möller, T., Harjula, R., Lehto, J. (2002) Ion exchange of ^{85}Sr, ^{134}Cs and ^{57}Co in sodium titanosilicate and the effect of crystallinity on selectivity. Sep. Pur. Technol. 28:13-23.

Onar, A. N., Akdemir, N. (2007) Effect of complexation on photocatalytic degradation of dissolved organic nitrogen compounds. Anal. Letters. 40:2949-2958.

Pekárek, V., Veselý, V. (1972) Synthetic inorganic ion-exchangers II. Salts of heteropolyacids, insoluble ferrocyanides, synthetic aluminosilicates and miscellaneous exchangers. Talanta 19(11):1245-1283.

Peyton, G. R., Glaze, W. H. (1988) Destruction of pollutants in water with ozone in combination with ultraviolet radiation. 3. Photolysis of aqeous ozone. Environ. Sci. Technol. 22:761-767.

Rekab, K., Lepeytre, C., Goettmann, F., Dunand, M., Guillard, C., Herrmann, J.-M. (2015) Degradation of a cobalt(II)-EDTA complex by photocatalysis and H2O2/UV-C. Application to nuclear wastes containing ^{60}Co. J. Radioanal. Nucl. Chem. 303:131-137.

Safarzadeh-Amiri, A., Bolton, J. R., Cater, S. R. (1996) Ferrioxalate-mediated solar degradation of organic contaminants in water. Solar Energy. 56(5):439-443.

Safarzadeh-Amiri, A., Bolton, J. R., Cater, S. R. (1997) Ferrioxalate-mediated photodegradation of organic pollutants in contaminated water. Water Res. 31(4):787-798.

Samuels, W. D., Camaioni, D. M., Babad, H. (1994) Initial laboratory studies into the chemical and radiological aging of organic materials in underground storage tanks at the Hanford Complex. In: Proceedings of Waste Management´94: working towards a cleaner environment, 1994, Tucson, AZ, United States.

Šebesta, F., John J., Motl, A., Rosíková, K. (2003) Study of combined processes for the treatment of liquid radioactive waste containing complexing agents. In: IAEA-TECDOC-1336 Combined methods for liquid radioactive waste treatment, Final report of a co-ordinated research project 1997-2001, IAEA, Vienna, Austria.

Seliverstov, A. F., Lagunova, Y. O., Ershov, B. G., Gelis, V. M., Basiev, A. G. (2009) Recovery of radioactive cobalt from aqueous EDTA solutions using concentrated ozone. Radiochem. 51(3):326-328.

Shannon, R. D., Prewitt, C. T. (1969) Effective ionic radii in oxides and fluorides. Acta Cryst. B25:925-946.

Slade, R. C. T., Hall, G. P., Ramanan, A., Prince, E. (1996) Structure and proton conduction in pyrochlore-type antimonic acid: a neutron diffraction study. Solid State Ion. 92(3-4):171-181.

Smičiklas, I., Dimović, S., Plećaš, I., Mitrić, M. (2006) Removal of Co^{2+} from aqueous solutions by hydroxyapatite. Water Res. 40:2267-2274.

STUK, ST1-5, accessed 15th August, 2019: https://www.stuklex.fi/en/ohje/ST1-5.

Stiepani, C., Bertholdt, H.-O. (2005) Full system decontamination with HP/CORD® UV for decommissioning of the German PWR Stade. In: Proceedings of 18th International Conference on Structural Mechanics in Reactor Technology (SMiRT 18), 2005, Beijing, China.

Tsuji, M., Kaneko, H., Tamaura, Y. (1993) Predictive evaluation of ion-exchange selectivity on a titanium antimonate cation exchanger. J. Chem. Soc. Faraday Trans. 89(5):851-856.

Wang, C. M., Heller, A., Gerischer, H. (1992) Palladium catalysis of O_2 reduction by electrons accumulated on TiO_2 particles during photoassisted oxidation of organic compounds. J. Am. Chem. Soc. 114:5230-5234.

Wang, G., Ling, Y., Lu, X., Zhai, T., Qian, F., Tong, Y., Li, Y. (2013) A mechanistic study into the catalytic effect of $Ni(OH)_2$ on hematite for photoelectrochemical water oxidation. Nanoscale 5:4129-4133.

Varga, K., Hirschberg, G., Németh, Z., Myburg, G., Schunk, J., Tilky, P. (2001) Accumulation of radioactive corrosion products on steel surfaces of VVER-type nuclear reactors. II. ^{60}Co. J. Nucl. Mater. 298:231-238.

Veselý, V., Pekárek, V. (1972) Synthetic inorganic ion-exchangers I. Hydrous oxides and acidic salts of multivalent metals. Talanta 19(3):219-262.

Yang, C., Xu, Y. R., Teo, K. C., Goh, N. K., Chia, L. S., Xie, R.J. (2005) Destruction of organic pollutants in reusable wastewater using advanced oxidation technology. Chemosphere 59:441-445.

Zachara, J. M., Smith, S., Fredrickson, J. K. (2000) The effect of biogenic Fe(II) on the stability and sorption of $Co(II)EDTA^{2-}$ to goethite and a subsurface sediment. Geochim. Cosmochim. Acta 64(8):1345-1362.

Zachara, J. M., Smith, S. C., Kuzel, L. S. (1995) Adsorption and dissociation of Co-EDTA complexes in iron oxide-containing subsurface sands. Geochim. Cosmochim. Acta. 59(23):4825-4844.

Zepp, R. G., Faust, B. C., Hoigne, J. (1992) Hydroxyl radical formation in aqueous reactions (pH 3-8) of iron(II) with hydrogen peroxide: The photo-Fenton reaction. Environ. Sci. Technol. 26:313-319.

Zouad, S., Jeanjean, J., Loos-Neskovic, C., Fedoroff, M. (1992) Structural study and thermodynamics of the fixation of strontium on polyantimonic acid. J. Sol. State Chem. 98(1):1-10.

Zouad, S., Jeanjean, J., Loos-Neskovic, C., Fedoroff, M., Piffard, Y. (1994) Sorption of strontium and lanthanum on polyantimonic acid and two phosphatoantimonic acids. J. Radioanal. Nucl. Chem, Articles. 182(2):193-204.